1-1-2013

Modeling HRTF for Sound Localization in Normal Listeners and Bilateral Cochlear Implant Users

Douglas A. Miller
University of Denver

MODELING HRTF FOR SOUND LOCALIZATION IN NORMAL LISTENERS AND BILATERAL COCHLEAR IMPLANT USERS

A Dissertation

Presented to

the Faculty of the Daniel Felix Ritchie
School of Engineering and Computer Science

University of Denver

In Partial Fulfillment

of the Requirements for the Degree

Doctor of Philosophy

---

by

Douglas A. Miller

August 2013

Advisor: Mohammad A. Matin

Author: Douglas A. Miller
Title: MODELING HRTF FOR SOUND LOCALIZATION IN NORMAL LISTENERS AND BILATERAL COCHLEAR IMPLANT USERS
Advisor: Mohammad A. Matin
Degree Date: August 2013

Abstract

Mathematical models can be very useful for understanding complicated systems and for testing algorithms through simulation that would be difficult or expensive to implement. This dissertation presents a model that attempts to simulate the sound localization performance of persons using bilateral cochlear implants. The expectation is that this model could prove to be a useful tool in developing new signal processing algorithms for neural encoding strategies.

The head related transfer function (HRTF) is a critical component of this model, and in the ideal case, provides the base characteristics of head shadow, torso and pinna effects. This defines the temporal, intensity and spectral cues that are important to sound localization. By building on the HRTF, a sound source localization model can be constructed.

This model was first developed to simulate normal hearing persons and validated against published literature on HRTFs and localization. The model was then further developed to account for the differences in the signal pathway of the cochlear implant (CI) user due to sound processing effects, and the microphone location versus pinna and ear canal acoustics. Finally, the localization error calculated from the model for cochlear

implant users was compared to published localization data obtained from these hearing impaired patients in order to validate the modified model.

Results of the normal hearing model correlated closely with localization performance data published in the literature, with localization error of the model only slightly greater than that of normal hearing subjects. The cochlear implant population has a more broadly distributed range of localization error than that of the normal hearing population, and in addition, the mean error is significantly poorer. The performance of the cochlear implant model fell within the range of error reported in the research literature for cochlear implant users. This close correspondence with the published performance data suggests that the model developed in this dissertation provides a reasonably good approximation of sound source localization for normal hearing subject and persons with bilateral cochlear implants.

Acknowledgements

I would like to express sincere gratitude to my academic advisor, Professor Mohammad Matin, for his guidance, support and friendship. His advice and critiques have been exceedingly helpful as I have pursued my graduate work here at the University of Denver. Also my earnest thanks and appreciation to Dr. Vija Narapareddy for presiding over my oral defense as Committee Chair, Dr. Matin for his direction and support as my Dissertation Director, and Professors Ron DeLyser, Mohammad Mahoor, and George Edwards for serving on my dissertation defense committee. Many thanks are due as well to the faculty, staff and fellow students of the School of Engineering and Computer Science. It has been a great pleasure to share in the camaraderie.

I am greatly indebted to my wife, Carol, and my daughters Tessa, Emily, and Laura, for their support, encouragement, and patience while I spent many hours working on this dissertation project. Their understanding, assistance and enthusiasm during these last few years were tremendously appreciated, and without which my doctoral studies would not have been possible. In addition, I thank my parents for their encouragement and best wishes in this endeavor.

Finally, I wish to honor the memory of Professor Roger Salters, who was an original member of my doctoral committee. His exceptional instruction and support were very influential during my academic studies. He will be greatly missed.

Table of Contents

List of Figures

List of Abbreviations

ACE	Advanced Combination Encoder (cochlear implant algorithm)
ANN	Artificial Neural Network
CAPZ	Common Acoustic Poles and Zeros
CI	Cochlear Implant
CIS	Continuous Interleaved Sampling (cochlear implant algorithm)
DTF	Directional Transfer Function
EABR	Electrically-evoked Auditory Brainstem Response
FFT	Fast Fourier Transform
FIR	Finite Impulse Response
HRIR	Head Related Impulse Response
HRTF	Head Related Transfer Function
IIR	Infinite Impulse Response
ILD	Interaural Level Difference
ITD	Interaural Timing Difference
JND	Just Noticeable Difference
KEMAR	Knowles Electronic Manikin for Acoustic Research
MAA	Minimum Audible Angle
RMS	Root Mean Square
SNR	Signal to Noise Ratio
SPEAK	Spectral PEAK (cochlear implant algorithm)
SPL	Sound Pressure Level

CHAPTER 1

Introduction

1. Overview

This work builds upon the author's previous master's degree work in that it continues to model the differences between the performance of cochlear implant (CI) users and that of normal hearing listeners. It is believed that this will help better understand the limitations of cochlear implants and will provide tools that may eventually prove useful in helping to develop better signal processing algorithms for neural encoding strategies in cochlear implants. In this dissertation, a brief introduction to the topic of this study is first presented. Then a statement of the problem and the purpose of this study are described. A literature review is provided for background of the research problem, and the public data and methods that were used in this study are described.

A mathematical representation of the auditory system's localization mechanism was developed and then realized using MatLab to create a model that could be used to process acoustic signals in order to extract localization information. Finally, this model was adapted from a normal hearing implementation to one representing typical cochlear implant signal processing algorithms. Both the simulated normal hearing and cochlear implant model were validated against published data from the research literature.

The core of the model developed in this dissertation is the human head related transfer function (HRTF). A number of techniques have been used by researchers to model the human HRTF and its impact on localization of sound. These models typically take into account head shadow and pinna (outer ear) effects, and their impact on interaural (between ear) spectral, timing, and intensity cues. A person with two normal hearing ears and an intact auditory nervous system uses these cues in order to localize the direction from which a sound is coming.

In contrast, users of bilateral cochlear implants have differing, more limited and degraded cues available to them for sound localization. This is due to several factors including, in current cochlear implant sound processors, that only some of the interaural intensity and time cues are maintained, the microphone is placed above and behind the ear such that cues from pinna and ear canal acoustics are lost, and the damaged nervous system may not be able to utilize all cues that are provided. The relative impact of differences in the physical cues received by the auditory system of the implant user versus differences in the ability of the damaged auditory nervous system to process the bilateral inputs is not yet clear and could benefit from further study.

2. Statement of the problem and purpose of the study

Problem:

To model the differences in localization ability between bilateral cochlear implant users and normal hearing listeners, some factors related to cochlear implant sound processing need to be considered. These include the fact that cochlear implant users have

differing head to microphone geometry and do not have the same pinna and ear canal effects as normal listeners, and that the signal processing of cochlear implants results in a decrease in bandwidth, a loss of frequency resolution, and degradation in some interaural cues. It is uncertain how much of the performance deficit of bilateral cochlear implant users is due to these factors versus that of central auditory processing deficits.

Hypothesis:

The poorer performance of bilateral cochlear implant users on auditory localization compared to normal listeners is primarily due to a combination of differences in the HRTF and degradation of the cues by the signal processing of the implants.

Purposes of the study:

To better understand the effect of the loss of physical cues due to cochlear implant signal processing on the auditory localization abilities of bilateral cochlear implant users compared to normal hearing subjects.

To help determine what effect the location of the cochlear implant sound processor microphone above the pinna has on the pole and zero trajectory of the HRTF as a function of source location, relative to the normal ear situation.

Study Approach:

This study was conducted in two parts, after the mathematical basis of the model was defined. First, a MatLab model was developed using the HTRF for the normal hearing listener, and this element was incorporated into a simulation of auditory

localization. The model was validated using published HRTF data from a KEMAR manikin[1], and against published localization data collected from normal hearing subjects. Second, the model was modified to test the hypothesis that the relatively poor localization performance of bilateral cochlear implant users is primarily due to a combination of factors including degradation of interaural intensity, and especially timing and spectral cues due to sound processor signal processing, and loss the of pinna and ear canal cues because of placement of the microphone. The resulting model was used to simulate the performance of bilateral cochlear implant users, and published data on sound localization by this population were compared to the simulated results of the model to test the hypothesis of this dissertation.

3. Background and literature review

Predicate modeling work

In previous modeling research conducted within the master's thesis of this author, simulated electrically-evoked auditory brainstem response (EABR) waveforms were generated for cochlear implant users through the use of an algorithm coded in MatLab. This model used as an input a unitary response derived through deconvolution of auditory brainstem responses in order to produce an EABR, as would be elicited in the brainstem of a person using a cochlear implant. In this previous work, a function vector was used to create a model of the combined firing of the neurons of the auditory nervous system. This

[1] KEMAR (Knowles Electronic Manikin for Acoustic Research) simulates average human torso, head, and pinna effects. It is often used as the standard in acoustic research.

combined firing is what is detected when conducting an EABR measurement, if a sufficient number of neurons are activated to elicit a measurable response. Additional equations were derived representing the latency and stimulus amplitude scaling functions present within the auditory nervous system. Other neural activity that can contaminate an ABR recording were also modeled, and combined with the simulated auditory brainstem response.

The responses generated by the MatLab model were often of better morphology and clarity than measured waveforms, but they had similar amplitudes and intensities compared with both published data and those empirically collected on the two subjects evaluated in that study. Even the threshold of response in the intensity functions was a reasonably good match to measured data (Miller and Matin, 2009), showing that MatLab modeling can be an effective method for understanding performance of cochlear implant users.

This earlier MatLab modeling work led to the author's interest in the localization model that is the subject of this dissertation. As with the earlier work, it is hoped that the localization model could prove to be a potentially useful tool for future cochlear implant research.

Normal binaural listening benefits

There are three primary effects ascribed to binaural listening in normal ears: the head shadow effect, the binaural summation and redundancy effect, and the binaural squelch effect (e.g. Durlach and Colburn, 1978). The latter two effects result in better

speech understanding due to the ability of the normal brainstem nuclei to fuse or integrate information arriving at each ear. Binaural summation refers to the fact that sounds presented to both ears rather than just one are actually perceived as louder, and binaural redundancy refers to improved sensitivity to fine differences in the intensity and frequency domains when listening with both ears rather than just one (e.g. Bronkhorst and Plomp, 1988). The binaural squelch effect (also called binaural unmasking) refers to the fact that the normal auditory nervous system is "wired" to help extract a desired signal out of loud background noise by combining timing, amplitude and spectral difference information from both ears so that there is a better central representation than would be had with only information from only one ear (e.g. Zurek, 1993).

In contrast to the binaural effects that require the central nervous system to use the information supplied, the head shadow effect is purely a physical phenomenon that is one component of the head related transfer function. It refers to the situation where speech and noise signals are coming from different directions (i.e. are spatially separated), so that there is always a more favorable signal-to-noise ratio (SNR) at one ear than at the other because the head attenuates sound. The amount of attenuation of sounds from the opposite side of the head is dependent upon frequency, impacting primarily frequencies higher than about 1500 Hz (Shaw, 1974) and ranging from about 7 dB through the speech range, to as much as 20 dB or more at the highest frequencies.

Both central nervous system integration and effects of the head shadow are involved in what is perhaps the most well-known practical binaural benefit, and the factor

studied in this dissertation, which is the ability to lateralize (left-right distinction) or localize (more fine gradients in the sound field). This function is dependent on auditory system perception of interaural differences in time, intensity, and phase (e.g. Yost and Dye, 1997). Interaural time differences (ITDs) provide the information necessary to locate the direction of low frequency sounds below about 1500 Hz (Shaw, 1974), while for sounds that are higher in frequency, the main cue for horizontal plane localization is intensity, called the interaural level difference (ILD) that occurs because of the head shadow effect (Yost and Dye, 1997).

The normal head-related transfer function (HRTF)

The HRTF refers to the characterization of the different time, spectral, and intensity cues for sounds arriving at each ear from different directions, due to a combination of effects on sound from the head, torso, and pinna. These provide interaural difference cues used for localization.

Figure 1 illustrates schematically how time of arrival and intensity differ at the two ears to allow a normal hearing listener to determine the direction from which the sound is coming. Duplex theory, first described by Lord Rayleigh in 1907, describes interaural time and level differences (ITDs and ILDs) for sound reaching the two ears as a function of that sound. As Figure 1 shows, the path from the source to each ear is different and in this example, the distance from the source to the left ear is greater than the distance from the source to the right ear. The difference in time that it takes the sound to travel to each ear is defined as the ITD. ITD is considered to be the most

prominent characteristic in determining where the sound source is located. It is however, usually not the only characteristic available for making that determination. As mentioned, there is the ILD, and there are also other factors that can be used. This is fortunate, as there are ambiguities that cannot be resolved through the analysis of ITD alone, and thus the necessity of analyzing these other cues.

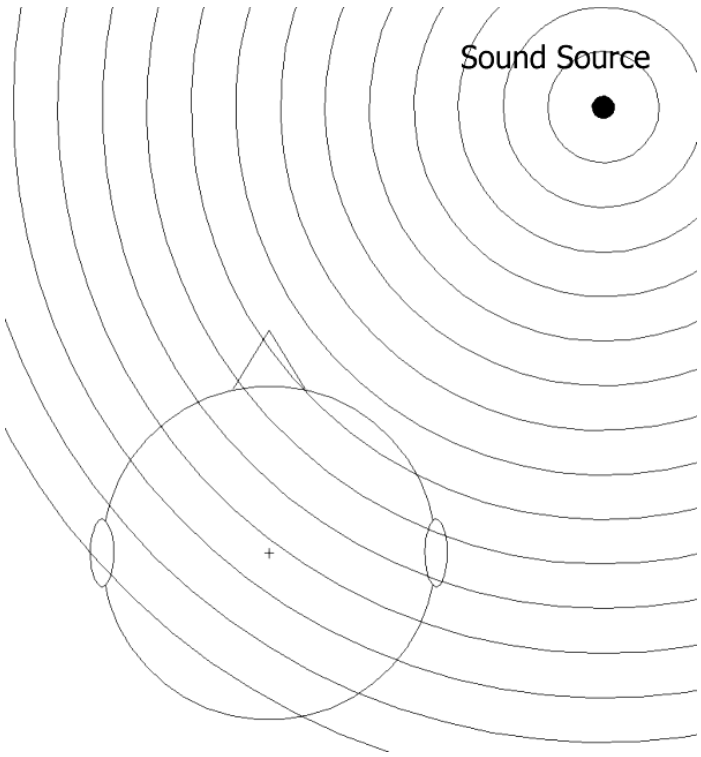

Figure 1. Diagram illustrating the time and intensity of sound arrival from a single source. It can be seen that the sound waves arrive later at one ear compared to the other, depending on the location of the sound source. Intensity is a function of distance from the sound source and therefore it is obvious that the intensity level will also be different. (from Miller and Matin, 2011)

If the sound source is permitted to vary in elevation and distance, as well as azimuth, then ITD and ILD cues do not necessarily allow the determination of a unique

location. This was first noted by Hornbostel and Wertheimer in 1920, when they described the locus of all points sharing similar ITD characteristics as resembling the surface of a cone (Figure 2). This set of points in space is often referred to as the "cone of confusion", since a sound source located at any of the points on this cone appears to be indistinguishable from the other points, as described by the duplex theory.

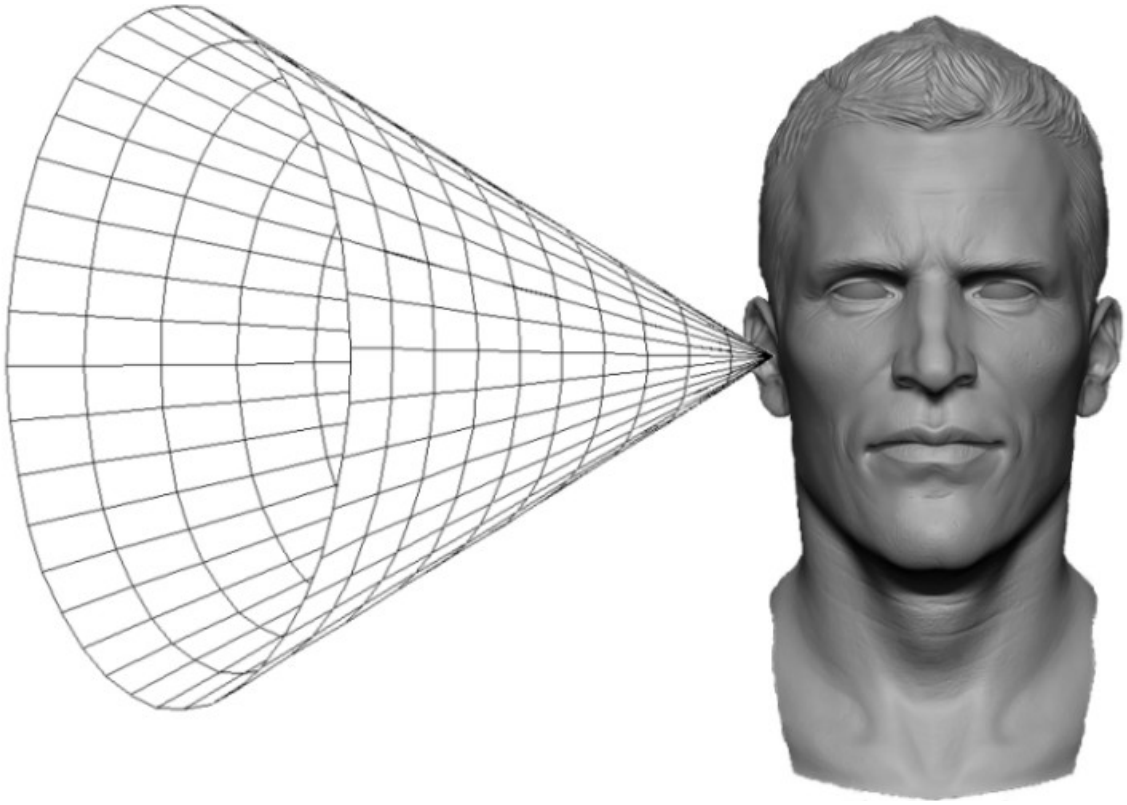

Figure 2. Illustration of the cone of confusion, the set of sound source coordinates that have the same ITD characteristics.

For a sound that has broad spectral content, pinna effects help to resolve the ambiguities of the cone of confusion. Sound resonating within the convolutions of the pinna is transformed and thus takes on differing spectral characteristics that vary

depending on the azimuth and elevation of the sound source. Certain frequencies are attenuated, creating spectral notches that provide additional auditory cues allowing improved localization of the sound source.

In order to extract these various auditory cues, the HRTF must be understood so that ITD, ILD, and other acoustic characteristics can be identified and analyzed. Figure 3 shows how the signal magnitude is affected over a range of frequencies as the signal source azimuth is varied (rotated about the subject).

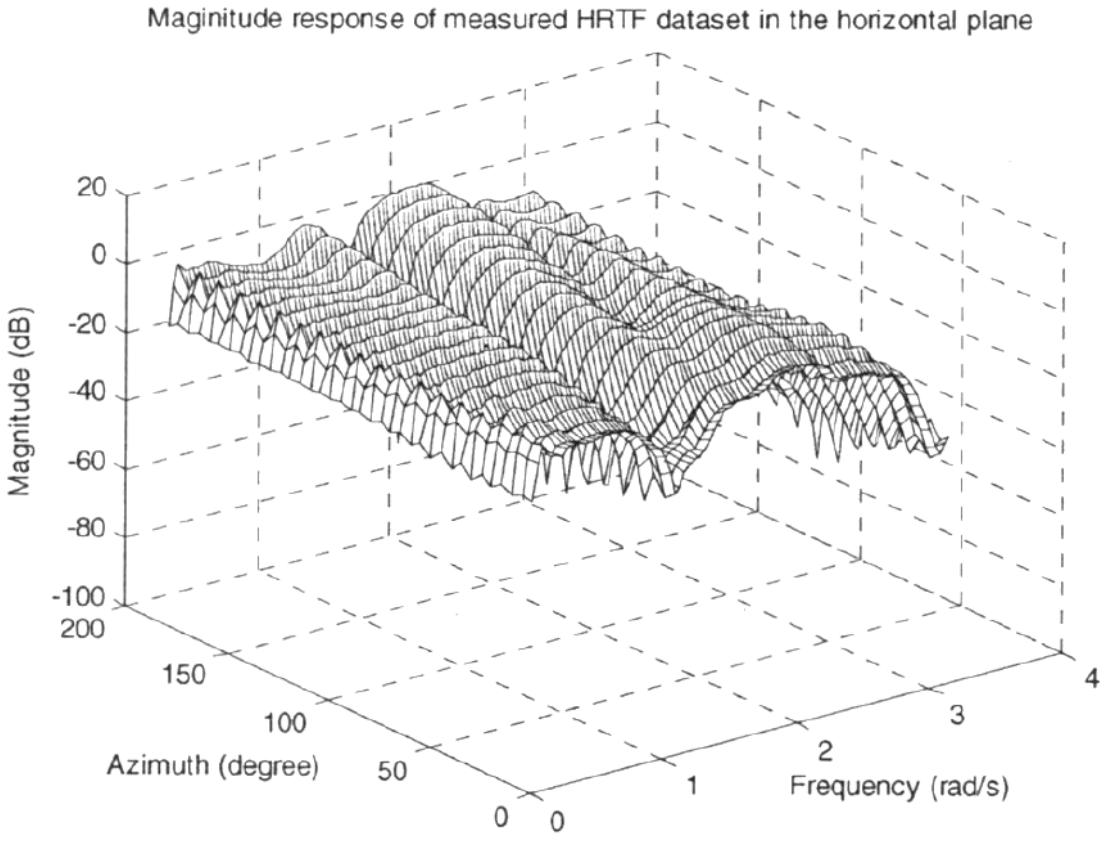

Figure 3. Magnitude response of the measured HRTFs on the horizontal plane. This depicts how the frequency response is shaped by head shadow, pinna and torso as the sound source is rotated about the body. (from Chanda and Park, 2005)

In this plot a characteristic notch in the frequency response is seen which has a linear relationship to azimuth. This relationship, which provides an important spectral cue and is often used in localization models, has come to be referred to as the first notch (FN) (Rice *et al*., 1992). Indeed, when examining the full spectral characteristics of the HRTF, it is found that there are multiple notches in the response. The first notch is a commonly studied feature, but one can see in the plot that there are others as well.

The literature on modeling of HRTF

There has been a great deal of modeling work of the HRTF conducted by various researchers, using a number of different techniques. Sometimes the simpler, directional transfer function (DTF) is used. The DTF is the direction specific component of the HRTF; that is, components of the HRTF that are the same for all directions are subtracted and what remains is the DTF. Some of the methods that have been developed for modeling the HRTF include:

- State space model (Adams and Wakefield, 2009)
- Geometric model (Algazi *et al*., 2002)
- Boundary source representation model (Bai and Tsao, 2006)
- Pole-zero approximation model (Blommer and Wakefield, 1997; Liu and Hsieh, 2001)
- Brown/Duda pole-zero model (Brown and Duda, 1997, 1998)
- Genetic algorithm model (Cheung and Trautmann, 1998)

- Fast multipole boundary element model (Gumerov *et al*., 2010; Kreuzer *et al*., 2009; Otani and Ise, 2006)
- Modeling by principal components analysis and minimum phase reconstruction (Kistler and Wightman, 1992; Scarpaci and Colburn, 2005)
- Infinite Impulse Response model (Kulkarni and Colburn, 2004)
- Interaural transfer function model (Lorho *et al*., 2000)

As an example, Faller *et al*. (2009) reported an initial stage in the development of customizable Head Related Impulse Responses[2] (HRIRs). Their goal was to develop a compact functional model that would be equivalent to empirically measured HRIRs, but that would require a smaller number of parameters obtainable from the anatomical characteristics of the test subject. To create this model, the HRIRs must be decomposed into multiple-scaled and delayed-damped sinusoids that would provide the parameters that the compact model requires in order to have an impulse response similar to the measured HRIR. Previously this type of HRIR decomposition has been accomplished through an extensive search of the model parameters. The proposed method approaches the decomposition simultaneously in the frequency (Z) and time domains. Although earlier methods had achieved a better fit than the method they proposed, several severe drawbacks with the earlier methods were observed. First, when the delay is small, the

[2] The Head Related Impulse Response (HRIR) is essentially the same as the HRTF. It is the output obtained when an impulse signal is applied to the HRTF.

second order STMCB[3] modeling method may inaccurately approximate the signal. Second, the average calculation time for previous methods was about 100 times longer than for the new method.

The authors suggested that it would be reasonable to recommend their inverse processing method for the creation of a large database, based on the separation of damped sinusoids according to the pole pair signature in the Z-domain. A large-scale study would be required, however, to establish the relationship between model parameters and the anatomical characteristics of individual subjects.

Applying HRTF models to studies of sound localization

One of the common purposes of HRTF models is to generate a virtual auditory environment through headphones, which can simulate sound source location for use in research. The models can also be used to predict performance in localizing various sound sources, as will be done with this dissertation. Research has been done using HRTF models as a component in simulation of the processes of localization cue encoding and extraction. These models include simulating one or more of ITD, ILD, HRTF, and DTF. ITD and ILD simply account for the difference in distance from the sound source to each ear, while HRTF and DTF also include the characteristic frequency shaping that occurs due the head shadow, pinna and torso reflections, and ear canal acoustics.

[3] The Steiglitz-McBride iteration (STMCB) is an algorithm for finding an IIR filter with a prescribed time domain impulse response.

Most of the work in the literature on auditory localization, both in normal hearing ears and in persons with hearing loss, has focused on performance for sounds in the horizontal plane rather than in the vertical plane (elevation), or in sound source distance discrimination. This is because the horizontal plane is most relevant to "real world" experiences of listeners such as determining which direction a car is coming from, or the location from which a person is calling to you. Thus, this dissertation will also focus on horizontal plane localization except for examining pinna effects, which also impact elevation perception.

Several researchers (e.g. Rao and Ben-Arie, 1996; Chung *et al*., 2000; MacDonald, 2008; Sen and Nehorai, 2009) have developed models based on HRTFs to simulate localization. For example, Chung *et al*. (2000) developed a computational model of auditory localization that resulted in performance similar to human subjects. The model incorporated cues available for sound localization using measured HRTFs, minimum audible field[4], and the Patterson-Holdsworth cochlear model to simulate the processes of auditory cue generation and encoding by the nervous system. A two-layer feed-forward back-propagation artificial neural network was trained to transform the localization cues into a two-dimensional map that indicates the direction of the sound source. The model results were compared with the localization performance of the subject who provided the HRTFs for the model and the mean localization performance of

[4]Minimal audible field is determined with the subject sitting in a sound field while the minimum audible stimulus is presented via a loudspeaker. The sound level is then measured at the position of the subject's head with the subject removed from the sound field. (Gelfand, 2009)

a group of 19 other subjects. The localization accuracy and front-back confusion error rates resulting from the model were similar to both the single listener and the group results. This suggests that the simulation of the cue generation and extraction processes as well as the model parameters were acceptable approximations of the biological system.

Birchfield and Gangishetty (2005) studied the possibility of using the ILD for acoustic localization by deriving constraints on the location of a sound source from the relative energy level of the signals received by two microphones. An algorithm was developed for computing the sound source location by combining likelihood functions for each microphone pair. They concluded that accurate acoustic localization can be achieved by normal listeners using ILD alone.

Kistler and Wightman (1992) measured HRTFs from both ears of 10 normal hearing subjects with sound sources at 265 different positions. They performed a principal components analysis of the resulting 5300 HRTF magnitude functions and demonstrated that the HRTFs can be modeled as a linear combination of five basic spectral shapes called basis functions. By assuming that HRTFs are minimum-phase functions and that interaural phase differences can be approximated by a simple time delay, they were able to model the HRTF phase. Subjects' judgments of the directionality of sounds that had been synthesized from modeled HRTFs and presented through headphones were nearly identical to their localization judgments of sounds synthesized from measured HRTFs. The authors concluded that their psychophysical results indicate

that the only cues needed for accurate localization in the horizontal plane are ITD and the ILD that are provided by the first basis function.

Each of the techniques developed has certain benefits and constraints, but the pole-zero model was chosen for this dissertation for several reasons. First, it is a continuation of previous work by another University of Denver engineering student who developed a model of the HRTF based on the movement of poles and zeros due to the source source's location.[5] In addition, pole-zero models have fewer parameters, which reduces the computational complexity.

If further reduction in computational complexity is required, a Common Acoustic Poles and Zeros (CAPZ) may be employed. This method utilizes a set of common poles, and only varies the zeros, simplifying the computations (Lui and Hsieh, 2001). In their work, Lui and Hsieh suggested that a set of HRTFs can be considered as a group of long-duration FIR filters, and this in turn can be approximated by using an IIR filter in place of each FIR filter. However, the CAPZ approach was deemed unnecessary due to the high degree of computational capacity in modern personal computers.

Bilateral Cochlear Implant Users

Present-day multichannel cochlear implants have proven to be a very successful treatment approach for patients who have severe to profound hearing loss, commonly

[5] Parametric Model of Head Related Transfer Functions Based on Systematic Movements of Poles and Zeros with Sound Location for Pole/Zero Models. A dissertation by Bahaa W. Al-Sheikh Hussein, 2009.

called “deafness”, in both ears (Parkinson *et al*., 2002). Over the last 30 years, the technology of cochlear implants has improved substantially and this is now considered the treatment of choice for patients meeting the criteria.

In audiology, bilaterally hearing-impaired patients have long been provided with hearing aids on both ears rather than just one ear because they perform better with sound input from both sides. In contrast, for many years cochlear implant candidates, despite deafness in both ears, were provided with only an implant on one ear. This was partly due to the cost of implantation surgery, insurers not covering more than one implant, and partly because early cochlear implants only provided minimal benefit to patients in the form of an adjunct to lip-reading skills. As the benefits of cochlear implants vastly improved over time, so that many cochlear implant patients had excellent speech understanding even without lip-reading, with most now even able to communicate comfortably over the telephone, it seemed reasonable to conclude that cochlear implant patients would also benefit from an implant on each ear. Balkany *et al*. published the earliest report of bilateral cochlear implants in an adult patient in 1988. The number of research reports in the literature on bilateral implant patient studies subsequently exploded over time (e.g. see reviews by Brown and Balkany, 2007, Papsin and Gordon, 2008, and Sammeth *et al*., 2011). The provision of bilateral implants today is becoming more commonplace, and there has also been a trend toward simultaneous implantation of both ears rather than sequential implantation (one at a time, with a varying period of time between surgeries). With the provision of bilateral cochlear implants, patients are now

realizing the benefits of binaural stimulation including the ability to localize sound source direction.

Potential benefits of bilateral cochlear implants versus unilateral

When hearing loss disrupts the ability of the brain to process binaural inputs, the benefits of two-eared listening are often severely degraded or even completely lost. A primary benefit of bilateral cochlear implants is that the ear with the more favorable signal to noise ratio (SNR) is always available, and overcoming of the head shadow effect for better speech perception in either quiet or background noise is considered to be a primary benefit of having an implant in each ear (e.g. Litovsky *et al*., 2006, 2009; Buss *et al*., 2008; Lovett *et al*., 2010). Binaural summation is known to occur in cochlear implant users with an implant on each ear because the amplitude has to be turned down to match the loudness perceived with only one implant activated. However, at this time the research literature indicates that only some bilateral cochlear implant users show evidence for true binaural redundancy effects on speech perception and even in those subjects, the benefit is smaller than that for the head shadow effect (e.g. Litovsky *et al*., 2006, 2009). This effect is probably not stronger in bilateral implant users either because such subtle cues are not able to be utilized by ears that have severe to profound hearing loss, or simply because the signal processing available in current-day cochlear implants (with two implants processing independently) does not adequately maintain the necessary interaural cues. Like binaural redundancy, there is also less robust evidence of improved speech understanding in noise in bilateral cochlear implant patients due to binaural squelch effects (e.g. Litovsky *et al*., 2006, 2009; Buss *et al*., 2008; Lovett *et al*., 2010).

Of significance to this dissertation topic, bilateral cochlear implant users are generally able to regain at least some ability to localize the direction from which a sound is coming relative to when they are listening with only a unilateral cochlear implant. This can be an important safety consideration, for example when they are crossing a busy street and need to know the direction that a car is coming from. Persons with only one cochlear implant also often complain of frustration when their name is called but they can't determine where the speaker is located.

Review of the cochlear implant literature on localization abilities

Bilateral cochlear implant localization research tasks have included either a simple left-right lateralization task (i.e., ± 90° azimuth) or use of a more complex set-up with numbered loudspeakers placed in a frontal arc, such as shown in Figure 4. The subject's head is kept stationary and faced forward, stimuli are presented from one loudspeaker location, and the subject identifies the loudspeaker he/she believes the sound came from (or in the case of infants or very young children, an observer identifies direction of head movement for right/left side discrimination). Multiple presentations and an adaptive procedure are used to determine the degree of accuracy in localization (e.g. Minimum Audible Angle [MAA] for a certain percent correct, or root-mean-squared [RMS] error). In some studies, presentation level is roved a few dB around a central value in an attempt to reduce monaural level cue comparisons at the two ears.

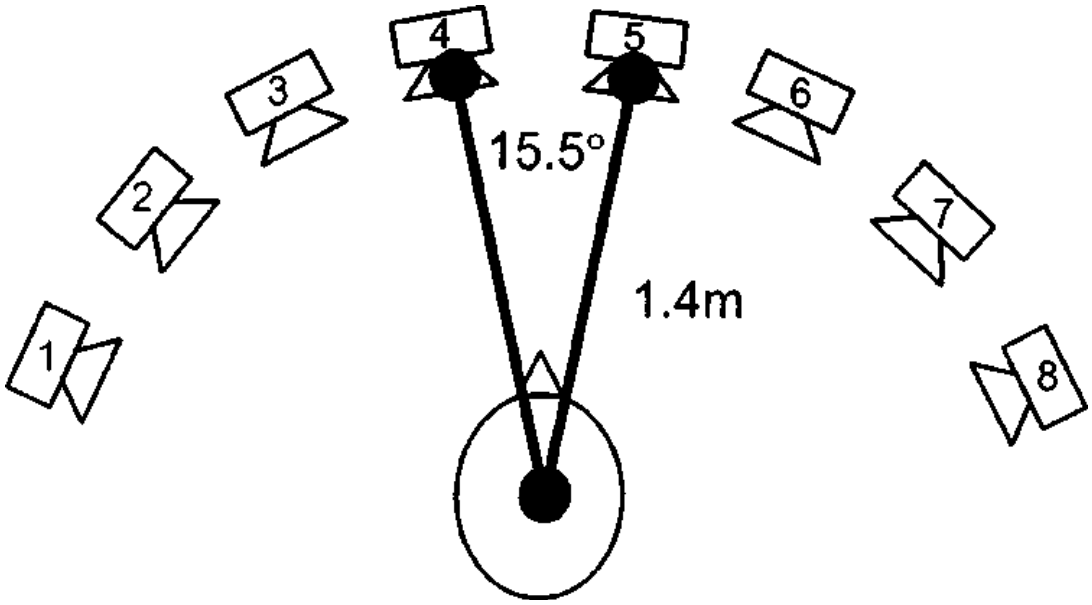

Figure 4. Schematic diagram showing a loudspeaker array used for horizontal frontal plane localization testing. (from van Hoesel and Tyler, 2003)

It is well known that interaural timing differences (ITDs) are of major importance in providing the information necessary to locate the direction of low frequency sounds less than about 1500 Hz (Shaw, 1974). For sounds that are higher in frequency, the main cue for horizontal plane localization is the interaural intensity level differences (ILDs) that occur due to the head shadow effect (Yost and Dye, 1997). For a listener with only one functional ear, there are very few cues to assist in sound localization. Tyler *et al*. (2007) reported on one unilateral cochlear implant user who was able to perform on a localization task as well as a typical bilateral user. They commented that the reason for this 'star' patient's good performance might have been that he was using spectral changes from head movements, or his knowledge that louder sounds were more likely from the implant side and sounds with less high frequency energy were more likely from the non-implant side. However, this kind of rudimentary localization ability is quite rare in a

unilateral cochlear implant user, and the vast majority of unilaterally implanted patients, or bilateral patients listening with only one of their implants, do not perform above chance level on localization tasks. When patients using bilateral cochlear implants are examined, however, the literature provides substantial evidence that localization ability is restored, albeit certainly not to the level of performance of normal hearing persons.

The earliest evidence was in the 1990s, when van Hoesel and colleagues (1993, 1995) showed that two adults with bilateral cochlear implants could effectively fuse the information from each ear for localization. Since then, other researchers have examined localization in larger numbers of subjects (e.g. Litovsky *et al*., 2004, 2006, 2009; Beijin *et al.*, 2007; Grantham *et al*, 2007; Buss *et al*., 2008; Dunn *et al*., 2008; Steffens *et al*., 2008; Mosnier *et al*., 2009; Tyler *et al*., 2002, 2003; Lovett *et al*., 2010; van Deun *et al*., 2010). Across these studies, test set-ups varied in terms of the number of loudspeakers (and thus the minimal audible angle), and there were also differences in subject factors and experimental designs. Despite this, however, across all the studies there appears to be a fairly striking result that, even though patients with bilateral cochlear implants perform below normal on localization tasks (e.g. Laske *et al*., 2009), they perform much better bilaterally than when listening with only one implant. The following provides a sampling of some of these studies.

In one early study, Tyler *et al*. (2002) collected data using a simple right-left lateralization task in seven patients who had been simultaneously implanted bilaterally. Loudspeakers were placed at 45° angles to the right and left of frontal midline and the

patient was asked to identify which loudspeaker produced a series of 3 pulses of speech-weighted noise (200 msec on, 200 msec off; 100 presentations per listening condition). Results revealed that most subjects had significantly better left-right discrimination using bilateral implants compared to using just one, as shown in Figure 5.

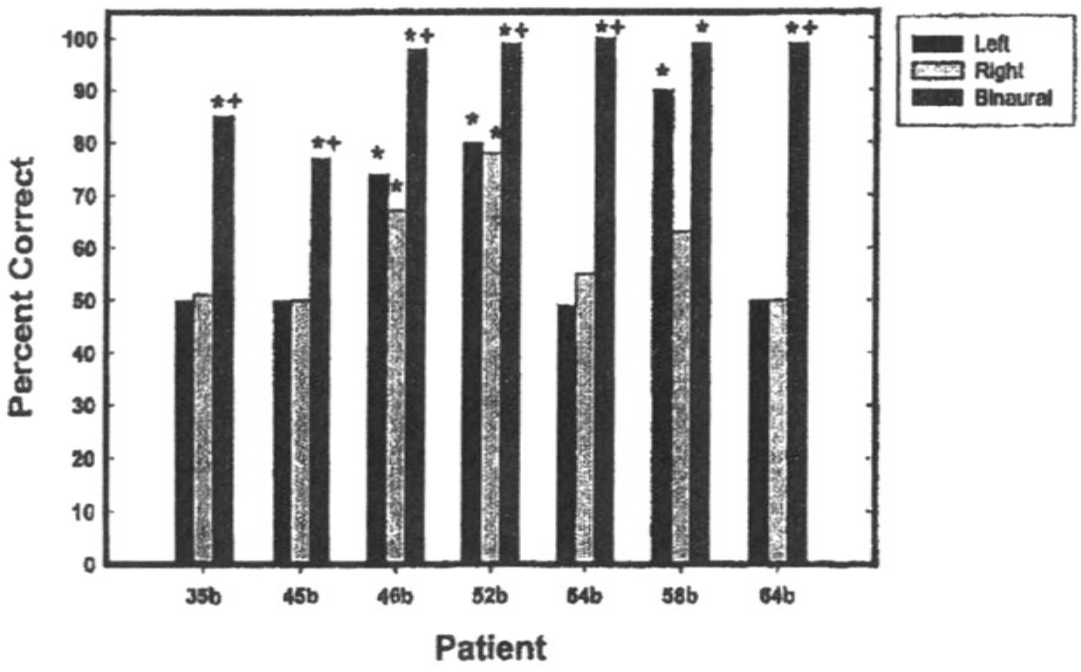

Figure 5. Left-right localization ability measured in the horizontal plane with two loudspeakers at ± 45° azimuth. Scores better than chance performance (50%) are indicated by an asterisk, and binaural performance significantly better than monaural (using binomial tests) is indicated by a plus (from Tyler *et al.*, 2002).

Horizontal plane localization measurements were taken on 16 bilateral implant subjects by Laszig *et al*. (2004). Using a 12-loudspeaker setup, 30° apart, short sentences were presented at conversational level. For 15 of the 16 subjects, and the group mean, performance was significantly better when listening bilaterally than when using either implant alone, with a reduction in the RMS degrees of error by 38°.

In 2005, Verschuur *et al*. examined localization ability in the horizontal plane of 20 adult bilateral CI users who had been sequentially implanted after < 15 years duration of deafness. Five stimulus types presented at between 60 and 70 dB SPL were used (speech, tones, noise, transients, and reverberant speech), with an 11-loudspeaker array. Results indicated a significantly lower mean localization error with bilateral listening (24°) than with unilateral (67°, with chance performance at 65°) . It was noted that this performance was still poorer than that of normal controls tested in a previous study (who averaged 2° to 3° localization error) or of typical bilateral hearing aid users (10° error). The authors hypothesized that the poorer performance of cochlear implant users was possibly due to the absence of temporal fine-structure cues in the processed stimuli, limitations associated with absolute level judgments due to amplitude quantization in the cochlear implants, or a poor ability to compare the amplitude spectrum between the ears limiting ILD perception. No large differences were found in performance across stimulus types or locations.

In 2003, van Hoesel and Tyler reported that the research literature showed that cochlear implant subjects typically have poorer performance than normal hearing subjects with an RMS Error for the cochlear implant subjects generally in the range of 10° to 30°. These researchers did report considerable variability, however, such that in exceptional cases 2° to 5° error was reported for a bilateral cochlear implant subject, while on the other hand, a very rare bilateral cochlear implant subject cannot localize acoustic signals at all.

In summary, the results across all these adult studies of localization in bilateral cochlear implant users provide strong evidence that localization is significantly enhanced with two implants compared to using only one, although the performances are still below those of listeners with normal hearing.

Direct examination of ILDs and ITDs in bilateral CI users

To directly examine the contributions of ILDs and ITDs, some researchers have examined performance of bilateral cochlear implant users with psychoacoustic studies of sensitivity (just noticeable differences, or "jnds") to ILDs and ITDs. In their 1990s series of studies, van Hoesel and colleagues (van Hoesel *et al*., 1993, 1995) conducted lateralization experiments to determine perception of right/left shifts with changes in stimulation to electrode pairs, one in each ear. Results showed that the subjects had good sensitivity to ILDs, but very large jnds in ITDs (about 0.5 to 1 msec) relative to normal ears. It was also noted that there were effects on ITDs of varying the electrical stimulation level between a patient's two implants. In 1997, van Hoesel and Clark found that jnds in ITDs were still large compared to normal ears even when place of stimulation on each side was carefully matched. Values were similar for stimulation rates from 50 to 200 pulses per second (pps), but increased at 300 pps.

In 2002, van Hoesel *et al*. looked at sensitivity to ITDs, and lateralization, in another adult bilateral cochlear implants user, using both two independent commercial sound processors, and custom laboratory software that allowed bilateral processing. Results with the clinical processors indicated substantial improvement in mean errors for

bilateral versus unilateral listening at 70 dB SPL (mean absolute errors of 80° and 73° for left and right ears versus only 16° for bilateral), and the custom bilateral processor produced comparable results. For measurement of jnds in ITDs using a 3-alternative forced choice task targeting 70% correct performance, the stimuli included simple low-rate electrical pulse trains and high-rate pulse trains modulated at 100 Hz. The jnds were about 400 μsec for rates between 50 and 200 pps for simple stimuli, which is substantially better than previous bilateral implant subjects they had tested, albeit still poorer than normal ears.

Later, van Hoesel and Tyler (2003) reported on five simultaneously implanted bilateral users. Lateralization studies indicated good sensitivity to ILDs down to 0.17 dB for some subjects, and sensitivity to ITDs on the order of 100 μsec. ITD sensitivity deteriorated when stimulation rates for unmodulated pulse trains increased above a few hundred Hertz, but at 800 pps showed sensitivity comparable to 50 pps when a 50Hz modulation was applied.

Laback *et al*. (2004) assessed the sensitivity of two bilateral cochlear implant users to ILDs and ITDs for signals presented through the auxiliary inputs of clinical sound processors that used a CIS sound processing strategy[6] (which preserves envelope cues but not fine timing information), and were configured to achieve equal loudness

[6] CIS is the acronym for Continuous Interleaved Sampling. This signal processing approach was developed by Blake Wilson and his colleagues at the Research Triangle Institute. This is the only coding algorithm that has been implemented by all three major CI manufacturers.

sensations at the two ears for diotic[7] input signals. In a lateralization experiment, jnds measured using a 2-alternative forced-choice method for ILDs indicated high sensitivity for the subjects for the broadband stimuli used, with values approaching those of normal hearing controls listening through headphones. Pitch-matched single electrode pairs showed lower jnds in ILDs than those for pairs of electrodes mismatched in pitch. The jnds in envelope ITDs were higher than those of the normal subjects and more variable on test-retest. The envelope ITD jnds for these two patients for click trains were lower than for a speech token or noise burst stimulus. The best envelope ITD jnd found was 259 μsec for the click train at 100 Hz for one of the subjects. Sound source lateralization results for the two hearing impaired subjects and two normal-hearing controls are shown in Figure 6.

In a Senn *et al*. (2005) study on horizontal plane localization, five sequentially implanted bilateral implant users were also evaluated for jnds in interaural intensity and time, using white noise bursts, click trains, and noise bursts in which either only the envelope or only the fine structure was shifted in time. The subjects showed near-normal interaural intensity jnds, but substantially poorer interaural time jnds than the normal controls. Envelope onset/offset cues could be perceived by these cochlear implant users but not interaural fine structure time differences.

[7] The term "diotic" refers to simultaneous presentation of the same sound to each ear.

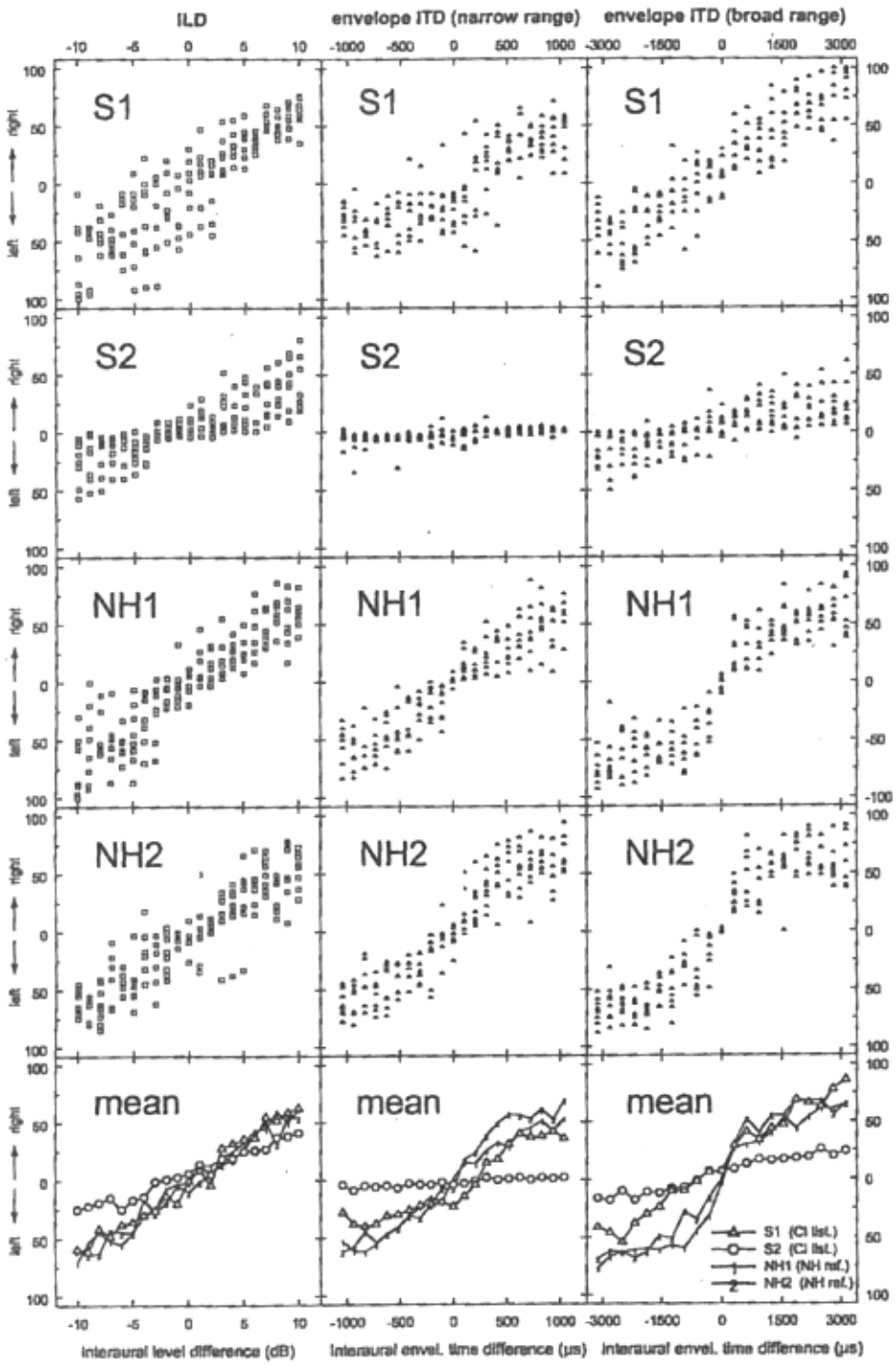

Figure 6. Lateralization judgments on ILDs (left column) and envelope ITDs within ± 1042 µsec (middle column) and within ± 3125 µsec (right column) for two bilateral cochlear implant users (S1, S2) and two normal-hearing controls (N1, N2). Bottom row summarizes the mean judgments for each listener. (from Laback *et al.,* 2004)

In summary, studies on bilateral cochlear implant users reveal overall a fairly consistent finding that they have much better sensitivity to differences in level between the ears than to differences in timing. This is consistent with the results of speech testing, which show a greater effect of head shadow (which is more dependent on ILDs) than of binaural squelch (which is also dependent on ITDs). There are also differences across stimulation rates, with sensitivity to fine-timing ITDs very poor in cochlear implant users for rates beyond a few hundred hertz.

Limitations of bilateral cochlear implants

The largest and most significant benefits in terms of speech intelligibility improvements with bilateral cochlear implants have been due to head shadow effects, and specifically to ILDs, while the effects of binaural squelch which are related to ILDs, but also to ITDs, are smaller when present. As noted by van Hoesel (2004), in order for bilateral CI users to obtain the same binaural advantages as normal listeners, sound-processing strategies of cochlear implants may need to preserve the appropriate ILD and ITD cues. In fact, according to van Hoesel, most current cochlear implants preserve only envelope timing cues (envelope ITDs) but not fine timing cues.

As noted by Tyler *et al*. (2003), there are several problems with trying to give more normal binaural hearing with cochlear implants. The first problem is that precise timing of interaural electrical stimulation is not yet possible with two independently functioning cochlear implants. This does not mean that bilateral coordination of pulsed signals is impossible, but it does mean that delay cues on a pulse-by-pulse basis may need

to be retained with some form of new signal processing if patients are to receive full benefit. A second problem is that, because binaural advantages depend on relative level information between ears, any cochlear implant processing system that modifies intensities and timing, such as with automatic gain control systems, might distort those cues. A third problem is that since cochlear implant patients have substantial numbers of missing cochlear hair cells and nerve fibers bilaterally, they may have developed abnormal binaural brain maps.

In his 2004 review, van Hoesel notes that even if signal processing schemes were developed to improve the contribution of timing information at the two ears, cochlear implant patients might not be able to hear or utilize these cues well due to poor sensitivity to small ITDs. Further, Wilson *et al*. (2003) in their review of the literature noted that results to date suggest that strict coordination of the carrier pulses across the two sides may not be necessary; i.e. lateralization is not impaired by different carrier rates on the two sides. What these researchers believe may be important is preservation of the relative timing and amplitudes of the envelopes across the two sides, as long as carrier rates are relatively high.

There has been a great deal of discussion in the literature regarding whether benefits from bilateral cochlear implants relate to some form of integration by the brain in the form of binaural squelch or binaural redundancy effects, or are merely due to the physical advantage of overcoming the head shadow. Although there is some evidence that true binaural signal processing can be seen in some bilateral cochlear implant users,

albeit sometimes only as a small effect, the most common benefit shown in the research literature is due to the head shadow effect. Clearly, however, the relative contribution of physical aspects versus neural processing to sound localization abilities of bilateral cochlear implant users is not yet well understood, and it is hoped that the results of this dissertation will help contribute to determining an answer to this question.

Model to examine localization in bilateral implant users

The MatLab model development for this dissertation simulated auditory localization ability in normal hearing listeners. It was further developed to simulate the impact on the auditory localization performance of bilateral cochlear implant users by imposing limitations of implant sound processing and supra-aural (above the pinna) placement of the sound processor microphone. In this way, it was possible to examine how much of the deficit in performance of bilateral cochlear implant users in localization compared to normal listeners is due to the physical characteristic changes in the cues provided to the central nervous system, versus problems in the central use and integration/fusing of those cues. The modified model was used to simulate the expected performance of bilateral cochlear implant users and then compared to results published in the research literature. This modeling work may also help to better understand how future cochlear implant sound processing should be modified to result in better sound source localization performance.

CHAPTER 2

Description of the Model

In order to describe the model, it is first necessary to lay some groundwork, including conventions and nomenclature. The angles of azimuth and elevation referred to throughout this dissertation are defined as shown in Figure 7.

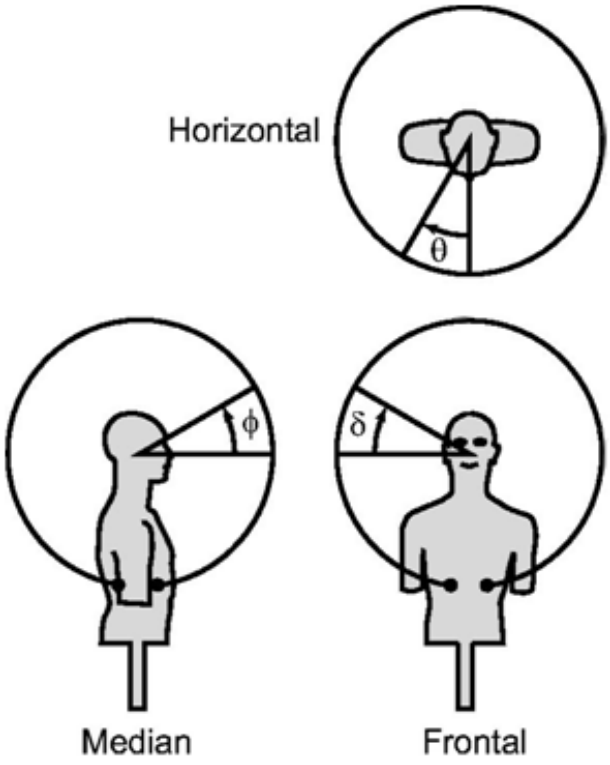

Figure 7. The coordinate planes as typically referred to in the study of sound source localization are the horizontal, median and frontal. The horizontal plane is most important in this model, as that is the plane in which azimuth angle, θ, is defined. Azimuth angle ranges from 0° to 360° (from Algazi *et al*., 2002).

The angle of elevation, φ, is often the only other angle used since azimuth and elevation can describe the vector to the sound source for any location. The angle depicted in the frontal plane, δ, is often not used since it is similar to φ in its usage. Azimuth is defined as the angle of rotation from the median plane in the horizontal plane, with median plane in front of the head being 0° and the median plane in back of the head being 180°. Elevation is defined as the angle above or below the horizontal plane. The median plane bisects the head left to right, and the horizontal plane is at the level of the ear. The frontal plane was not deemed to be needed for defining any elements of the model, and was therefore not used in this study.

Other nomenclature used within this work includes "ipsilateral" and "contralateral". For the purposes of this study, the ipsilateral ear is the side of the head on which the sound source is located, while the contralateral ear is the opposite side of the head.

1. Mathematical basis

The foundation of the model is based on the head related transfer function (HRTF) algorithm. The MatLab model includes the most significant aspects of the HRTF that represent the pinna and head shadow effects. A block diagram of the general HRTF is illustrated in Figure 8. This is a simplified representation of Brown and Duda's work that also includes room effects. The room effects element was not implemented in this work, as the environment was assumed to be anechoic.

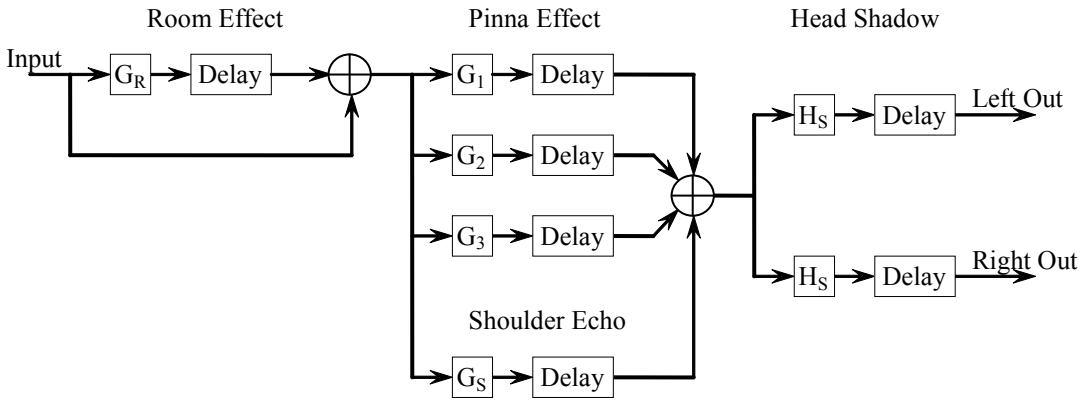

Figure 8. Block diagram of the head related transfer function algorithm (based on Brown and Duda, 1998).

This block diagram can alternatively be expressed in the form of brief descriptions of each step in the process. In a simplified form the basic algorithm for sound source location estimation is as follows:

- Filter the signal as appropriate in order to account for head shadow and pinna effects or a cochlear implant processor
- Compute FFT of the resultant signal in order to extract the magnitude and phase components
- Identify dominant components regarding localization cues
- Compute phase difference to extract the ITD
- Using a vector model, determine the azimuth
- Following determination of the detected azimuth, compare this to the actual source azimuth

Head Shadow Effect:

This component is responsible for generating the ITDs and ILDs caused by the shadowing effects of the head, which primarily impact high frequencies due to their small wavelength relative to the size of the head. ITD for a particular frequency is determined as follows:

$$ITD = \frac{cT_D}{f} \tag{1}$$

where c is the speed of sound, T_D is the time difference of the signal's arrival, and f is the frequency of interest. This part of the model is very similar for both normal ears and cochlear implant users.

The first element of the algorithm is a simple pole-zero filter which is meant to approximate the Rayleigh spherical head model. It is parameterized by the angle difference between the location of the ear and the azimuth of the sound source.

The gain of low frequency signals (below about 1500 Hz) is not drastically affected by head shadowing due to their larger wavelengths. To achieve this effect, the head shadow model has a fixed pole and a zero that moves to produce the desired amount of roll-off, depending on the azimuth of the sound source.

As part of the head shadow component there is a linear delay element. This accounts for the ITD produced by the waves propagating around a rigid sphere to reach the ear.

The pole-zero filter suggested by Brown and Duda (1997; 1998) in their model is given by:

$$H(\omega) = [1 + j(d\omega)/(2m)] / [1 + j\omega /(2m)] \quad (2)$$

where:

$$m = \frac{speed\ of\ sound}{radius\ of\ the\ head}$$

and $d\omega$ is derived from:

$$d(\theta) = 1.05 + (.95 * \cos(1.2*\theta)) \quad (3)$$

where θ is the angular difference between the location of the ear and the azimuth of the sound source.

The linear delay element for each ear (in seconds) is given by:

$$T(\theta) = \begin{cases} -\frac{\cos(\theta)}{m}: & 0° < |\theta| < 90° \\ \frac{|\theta| - 90}{m}: & 90° < |\theta| < 180° \end{cases}$$

Figure 9 is a graphical depiction of how results are generated by the model in this implementation. This is the basic algorithm that derives the ITD aspects of the HRTF that will significantly affect the accuracy of the localization prediction.

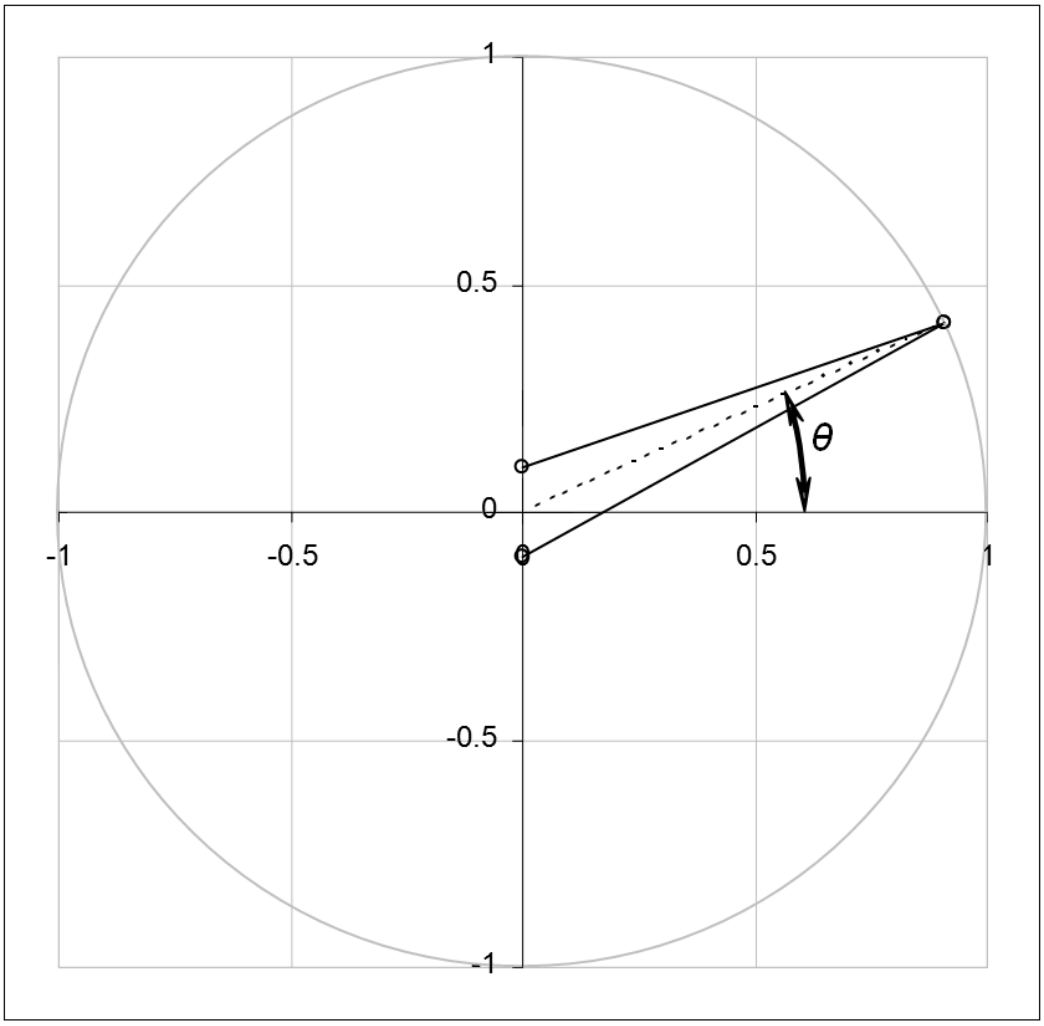

Figure 9. The solid lines represent the vectors corresponding to the signal paths from the target to the two ears. The dashed line represents the angle computed from the phase difference of the signal acquired at each ear. (from Miller and Matin, 2011)

Pinna Effects:

Brown and Duda's approach (Brown and Duda, 1998) to developing a pinna model was to work only in the time domain. Their primary reason for working in the time domain is that many of the characteristics of HRTFs are a consequence of sound waves reaching the ears by multiple paths. Sound that arrives over paths of different lengths interact in a manner that is obscure in the frequency domain, but is easily understood in the time domain. This greatly simplifies the structure of the model and reduces the computational requirements in implementing it.

Pinna effects dependent on the sound source's azimuth are essentially caused by a series of echoes reflecting off of the surfaces of the pinna and into the ear canal. Like azimuth, the elevation of the sound source also affects how the sound waves reflect off of the pinna, and thus compound the effect. If a relationship can be found between the azimuth and elevation of the sound source and the characteristics (time delay and amplitude) of the most important echoes resulting from the pinna geometries, a transfer function that represents this part of the system can be determined and incorporated into the model.

As can be seen in Figure 10, there are various folds and ridges of the pinna which create differing reflections of the sound waves. Indeed, these are different for each person, but for the purposes of this research, an idealized pinna as represented by the KEMAR manikin is used.

As a side-note, torso effects, also referred to as shoulder echo, were examined during this course of study and were found to have little significance in localization performance. In fact, performance with and without the shoulder echo was compared in the normal hearing model and mean error remained unchanged. This element was therefore dropped from the model in order to decrease computational time and to reduce complexity of the model.

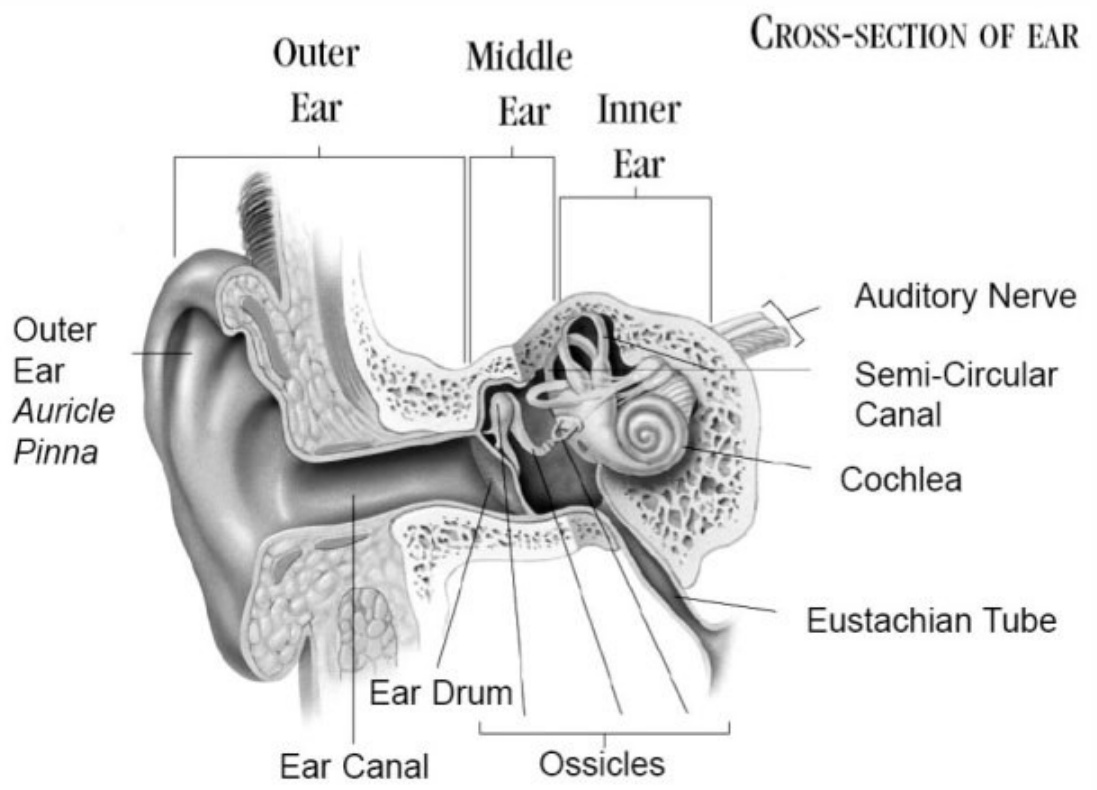

Figure 10. Cross-section of the ear showing the features of the pinna which are responsible for the echoes and delays that affect the sound waves as they enter the ear canal (obtained from http://tekupengahauora.org.nz/services/ear-health.html).

Cochlear Implant Processor Effects:

Because the microphone of the ear-level sound processor for a cochlear implant user is placed above the pinna, the same pinna effects are not present as for a normal listener wherein the pinna acts as a funnel to send the sound down the ear canal to the tympanic membrane. Thus the pinna effects must be modeled differently. Figure 11 describes the block diagram of the HRTF of the cochlear implant model. The pinna effects are eliminated or much simplified for the cochlear implant case, as a minimal number of reflections introducing only very short time differences are required for the model. Since the pinna effects on the microphone response are relatively small compared to the signal transformations produced by the cochlear implant processing, these were neglected for this iteration of the model.

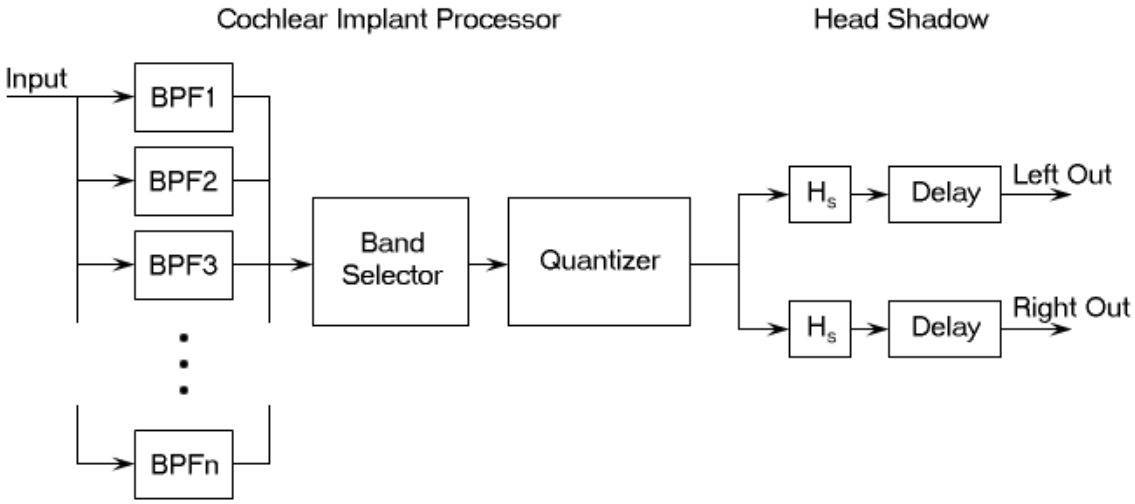

Figure 11. Block diagram of the head related transfer function for the cochlear implant model. It can be seen how the pinna effects are replaced by the cochlear implant processing functions, as compared to the normal hearing model.

Another aspect of cochlear implant signal processing that must be represented in the model is spectral and intensity quantization that occurs. The bandpass filter bank covers the entire spectral range of speech, but the processing algorithm only selects those filter bands that have the greatest energy. There is further reduction in accuracy of the signal as the energy levels of the bandpass filters are quantized by the processor during analog-to-digital conversion.

In conclusion, the model that is the topic of this dissertation includes assessment of the impact of the head and pinna effects in normal hearing persons, and the differences in the physical configuration for bilateral cochlear implant users because of placement of the sound processor microphone. Also considered are the degradations in spectral and intensity cues due to the signal processing performed by the cochlear implant. A comparison of these differences was an important aspect of the model development.

CHAPTER 3

Methodology

1. Overview

The measurement of individual head related transfer functions (HRTFs) can be quite expensive and time-consuming. Typical requirements include an anechoic chamber and high quality audio equipment, including an array of high fidelity speakers arranged such that the signal can be delivered from any direction. In order to make acoustic spatialization technology more widely available, generic HRTFs have been developed and used (although they do not work as well as individualized HRTFs). Once determined, HRTFs are convolved with the sound signal in order to give it a directional characteristic.

For this work it is desirable to develop a signal processing model for HRTFs that is able to be efficiently implemented on modern microprocessors. An ideal model would contain all of the important spectral features of an HRTF that are used for localization. However, in the interest of developing this model with more moderate resources, average human head data as simulated by a KEMAR manikin was used, and these are expected to provide reasonably accurate parameters for the model. A KEMAR manikin like the one used for collecting the HRTF data by the Media Laboratory of the Massachusetts Institute of Technology is shown in Figure 12.

The HRTFs for each ear were recorded through the two microphones placed in the head of the manikin. These microphones are situated so that they pick up the acoustic signal at the location of the acoustic membrane (commonly referred to as the ear drum).

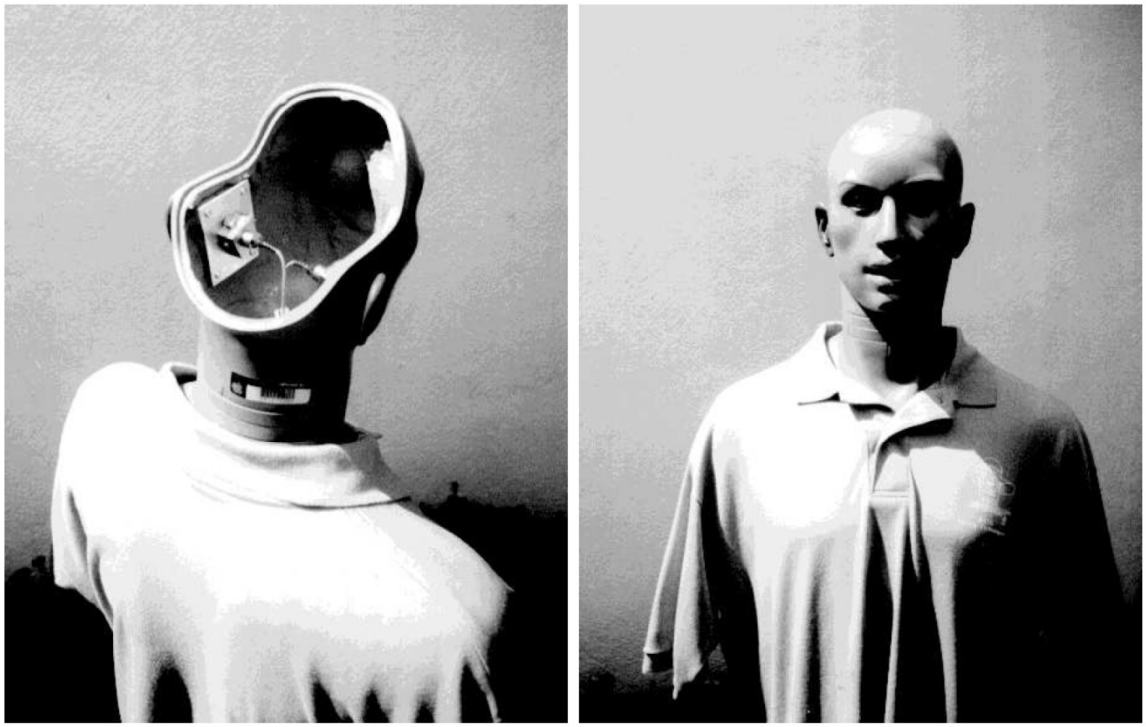

Figure 12. The KEMAR manikin showing how the recording microphones are placed within the head so that they can pick up the acoustic signals entering through each pinna. (from Duda, 2000)

The plots depicted in the following figure (Figure 13) shows the HRTF from the KEMAR manikin that were used in this model development. This family of curves represents the signal at the ear for all azimuths as the sound source is rotated around the head at a fixed distance. The raw data from both ears for a signal located in the horizontal plane were obtained from the MIT lab's publicly available archives.

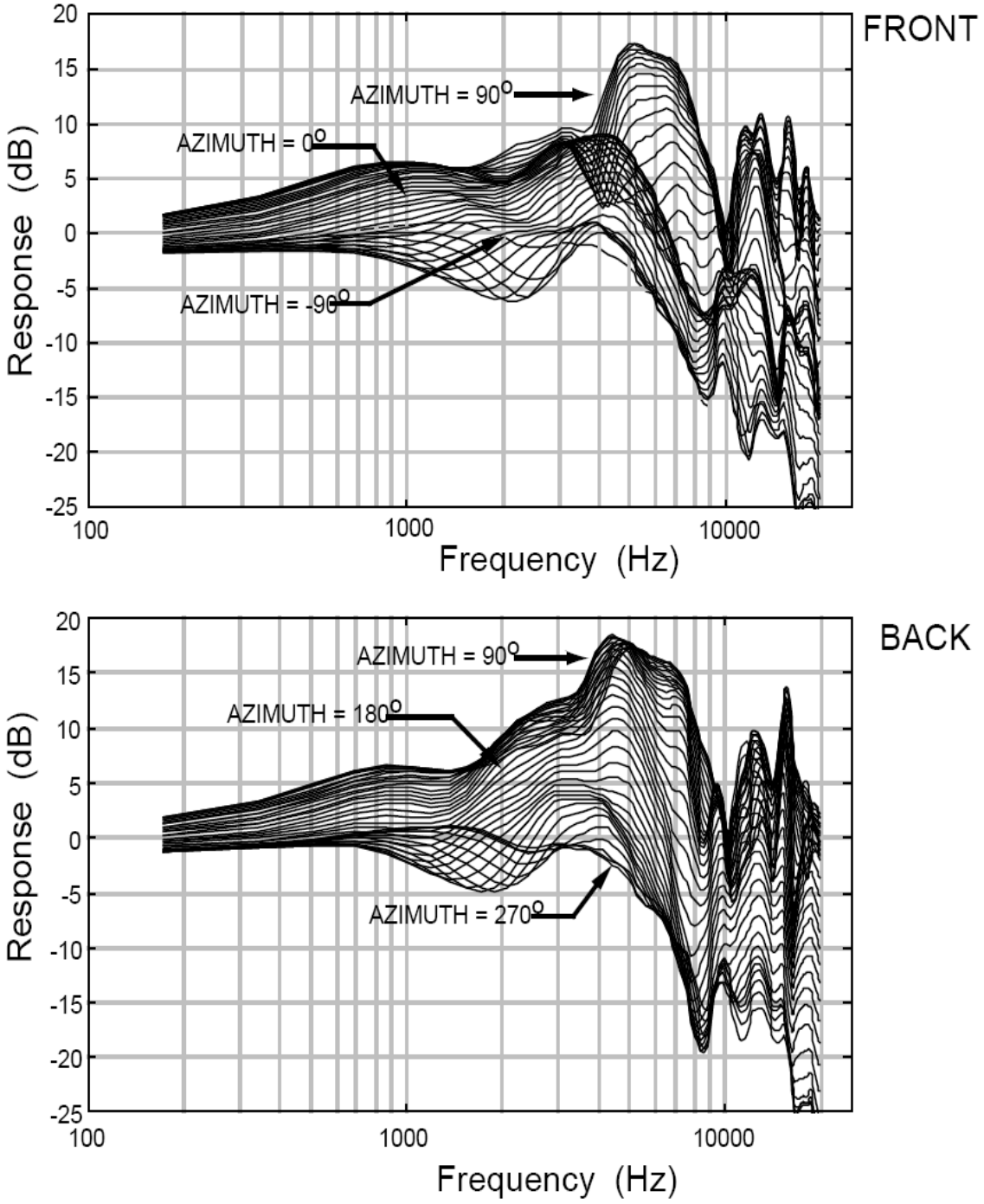

Figure 13. The right ear HRTF from a KEMAR manikin obtained in the horizontal plane. The same recordings were also collected for the left ear. (from Duda, 2000)

2. Computer modeling of the normal HTRF using MatLab

To begin, the model was built based on a spherical-head model (the most basic model) and then other influences were added to the model and finally a pole-zero approximation was applied to increase the overall accuracy. HRTFs can be convolved with a monaural sound in MatLab to produce the signals supplied to each ear. This represents the basic normal listener model. The HRTFs can then be modified to make them more effectively represent a particular condition, i.e. performance of a person with cochlear implants. Published data on individual HRTFs reveals how they change with the shape of the head, torso and pinna. By extrapolating this information, it is possible to alter the transfer functions to represent the cochlear implant case.

This model contains three main components. Because this is a linear system, the order of the components does not matter in the actual implementation. The first element representing the head shadow effects will produce the ITDs. The second element represents the filtering effects of the pinna and also incorporates the gain representing the ILDs. The azimuth of the sound source can be accurately determined with ITDs and ILDs. The third element represents echoes from the pinna that cause spectral filtering. This element also incorporates the information related to the reflections caused by varying azimuth and elevation that alter the spectral filtering parameters.

3. Analysis of the model

There is a large repository of HRTF data acquired from a KEMAR manikin that was collected by Gardner and Martin at the Massachusetts Institute of Technology

(Gardner and Martin, 1995). These data are freely available for research purposes and validation of the HRTF component of the normal model was conducted using this information.

The simulated results from the model were also compared against available published performance data on localization for a group of normal hearing subjects. The data set used for this latter purpose was combined from several published data sets in the sound localization research literature.

4. Computer modeling of the cochlear implant HTRF using MatLab

The base model developed for normal hearing was created in a modular fashion in order to simplify incorporating cochlear implant emulation. The pinna effects were incorporated into the normal hearing model by creating it as a separate function in MatLab. This made it a simple matter to remove the pinna effects and replace that MatLab function with one that represented a cochlear implant processing algorithm.

Cochlear implants place a signal processor in an externally worn unit that fits behind the ear. The signal processor also contains the power source, and microphone, as illustrated in Figure 14. The component labeled (1) is the external processor where the signal is transformed prior to being sent on to the implant, labeled (2). The algorithm that processes the acoustic signal is stored in memory in the external processor, and is therefore easily updated with another algorithm, if so desired.

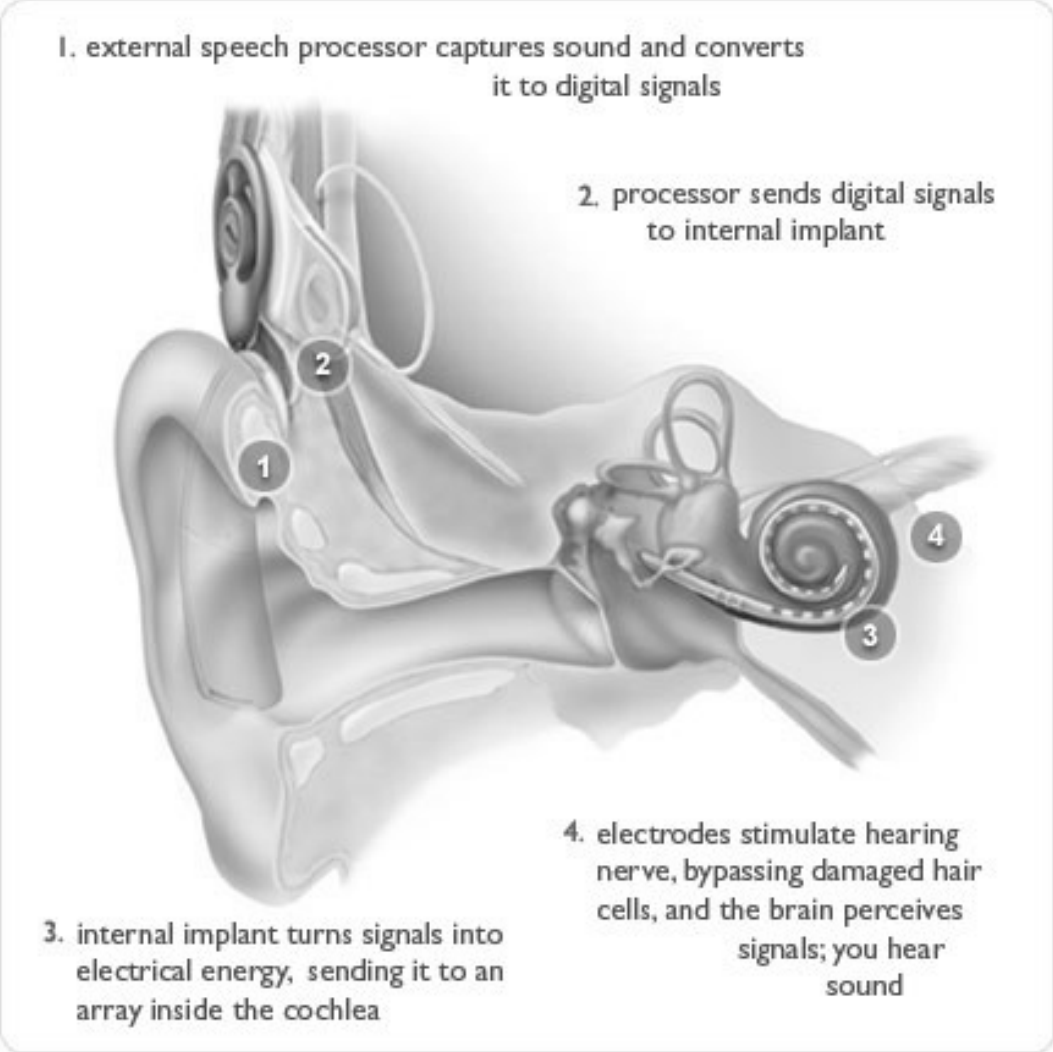

Figure 14. Illustration of how the cochlear implant restores the sensation of hearing for the severely to profoundly impaired ear. (courtesy of Cochlear Limited, Sydney, Australia).

In a typical cochlear implant sound processing algorithm, the acoustic signal is obtained from the microphone of the external processor and bandpass filtered with a filter bank such that the signal is spectrally segregated into a number of filter bins (there are 22 filter bins in the ACE implementation), as described in Figure 15. The filter bins are then analyzed, and the bins containing the most energy are selected (four in the ACE algorithm). The electrodes corresponding to these selected bins are then sent electrical

impulses, each scaled to represent the amount of energy in the associated bin. This is the basic structure of the Advanced Combination Encoder (ACE) and Spectral Peak (SPEAK) (which uses only 20 filter bins) algorithms that are in common use with the Nucleus 24 cochlear implant (Vondrasek *et al*., 2008). The model that is the subject of this dissertation is based on the sound processing algorithm that is most commonly used in cochlear implants today, namely the ACE approach.

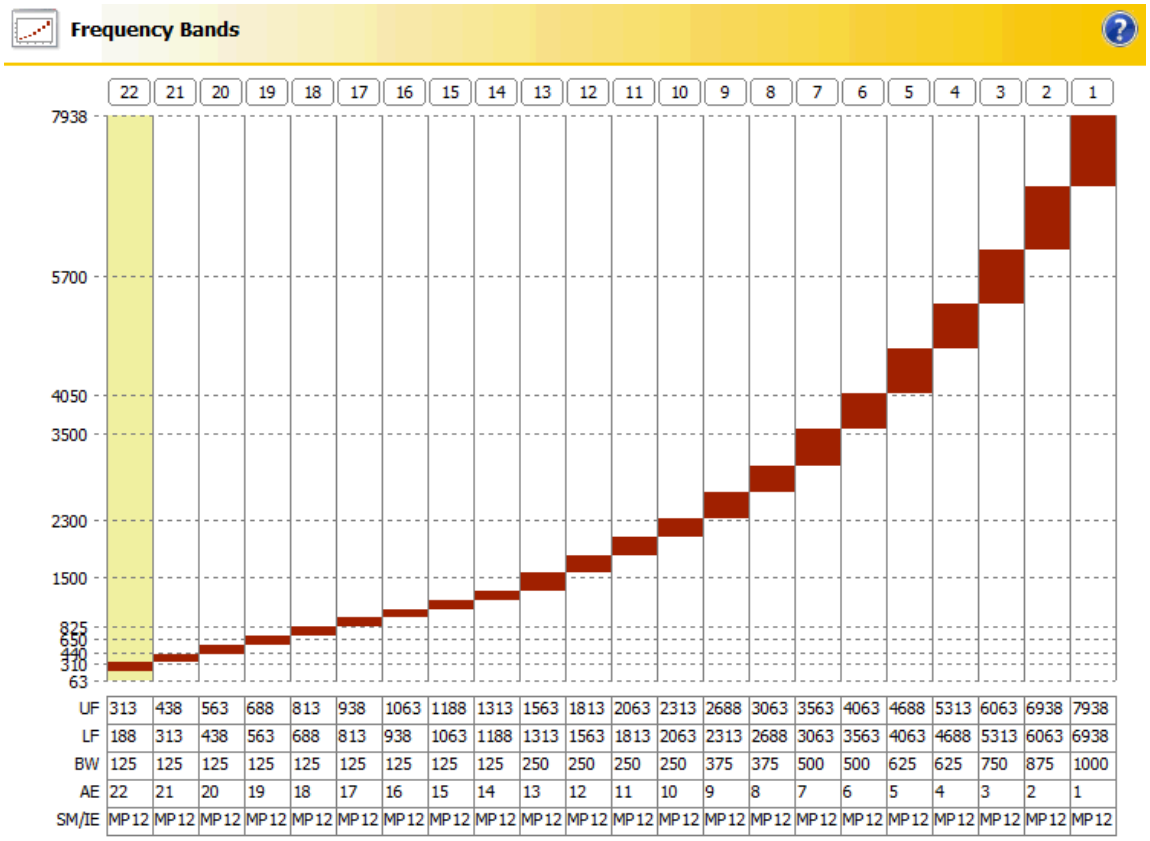

Figure 15. Frequency Allocation Table for typical programming of a Nucleus 24 cochlear implant. (Source: Custom Sound programming software, Cochlear Limited, Sydney, Australia)

The cochlear implant model developed herein mimics this by filtering the signal in a similar manner before applying the localization algorithm. As developed in this model, the signal is segmented into 22 frequency bands, as illustrated in Figure 15 following the algorithm used by the cochlear implant processor, and the four bands containing the greatest amount of energy are selected. The transformed signal is then returned to the sound source localization function for determination of the azimuth.

5. Statistical methods

A statistical method commonly used in the evaluation of human localization performance is that of root mean square (RMS) error analysis of the difference between the actual azimuth of the signal source and the detection angle obtained from the test subject's response.

RMS Error is determined by:

$$RMS\ Error = \sqrt{\frac{\sum_{i=1}^{n}(\hat{y}_i - y_i)^2}{n}}$$

where $\hat{y}$ is the predicted value and y is the observed value.

RMS Error values for normal hearing and cochlear implant subjects' localization abilities were obtained from the literature for comparison to the model's localization performance. The signal data from azimuths ranging from 0° to 180° in 5° steps were input into the model for both normal hearing conditions and cochlear implant conditions

and the error at each azimuth was calculated. An RMS Error was then computed for each data set for comparison to published mean error values. A comparison of each data set by azimuth angle would also be desirable; however, the published studies did not include the data required to make this comparison.

CHAPTER 4

Normal Hearing Model

1. Results for the normal hearing model

Following construction of the basic model elements in MatLab, acoustic signals were fed into it to assess their performance. Some results from the modeling work representing the head shadow effect are presented in Figure 16 and Figure 17. These are the magnitude and phase plots representing the HRTF for KEMAR. They were derived by Fourier transforming the acoustic data obtained from KEMAR by the Massachusetts Institute of Technology laboratory of Gardner and Martin (1995).

The acoustic source data consisted of Maximum Length Sequences[8] of 16384 bit length played through a loudspeaker and recorded through the KEMAR ears. These plots represent the HRTF derived from these data. The surface plots depict the magnitude of the transfer function over azimuths of 0° to 180°. Note that 180° to 360° are a mirror image, and thus are merely a transposition of the left and right responses. This is evident if one joins the 0° edges and 180° edges of the left and right magnitude plots.

[8] Maximum Length Sequences are pseudorandom binary sequences commonly used for measuring acoustic characteristics due to their spectrally flat nature and because they provide recordings that are highly immune to external noise.

The notches in the response that were characterized by Rice *et al*. (1992), and which were discussed in Chapter 1, can be clearly seen in the magnitude surface plots of Figure 16. The first notch is plainly visible at around 8000 Hz to 10,000 Hz, and a prominent second notch is seen at about 15,000 Hz. These are representative of the pinna effects and are key characteristics in sound source localization. Clearly there are additional, less prominent characteristics in the response that are also available for more finely resolving sound source direction.

The Fourier transformation of the HRTF also provides the phase angle of the signal, key to determining the interaural timing difference (ITD). The phase plots in Figure 17 depict the phase calculated from the transfer function for each ear. The phase values extracted from the HRTF are used in the model for the first order approximation of the azimuth angle to the sound source.

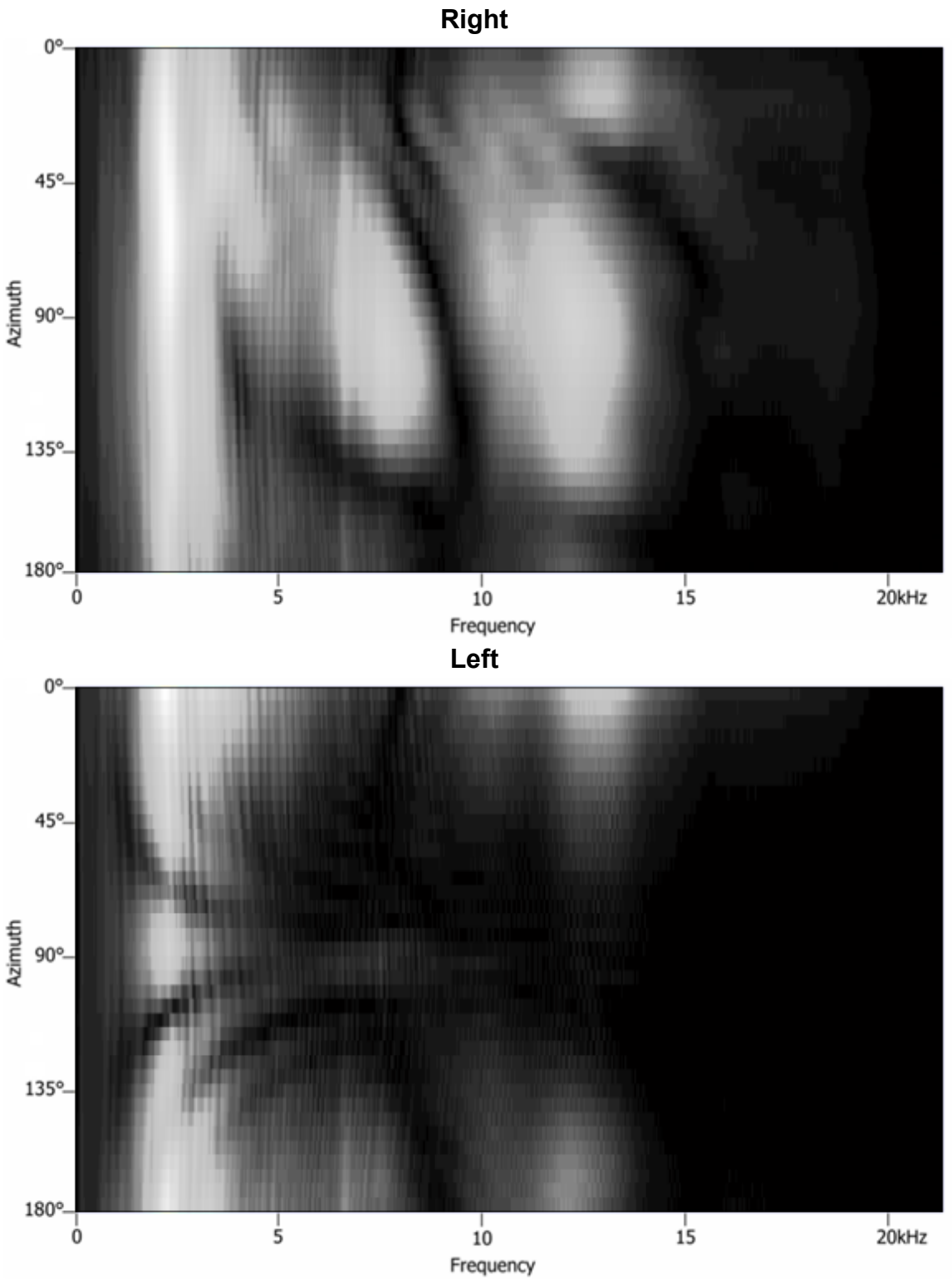

Figure 16. Signal magnitude obtained at each ear as azimuth is varied between 0° and 180° (right is the ipsilateral ear and left is the contralateral). The color represents intensity, with black corresponding to low signal strength and white corresponding to high signal strength.

In Figure 17 the phase angles for the ipsilateral ear and contralateral ear are presented with 0° azimuth indicated with the heavy red line. It can be seen that there is an orderly progression of the phase angles towards lesser values as azimuth is changed from 0° to 90° in the ipsilateral ear. Conversely, the phase angle increases, but also in an orderly manner, in the contralateral ear.

These phase angle progressions with change in azimuth result in a phase differential that is 0° for 0° azimuth, and increases as azimuth approaches 90°. The phase angle differential reaches its maximum at 90° azimuth, and then decreases back to a phase differential of 0° at 180° azimuth.

Therefore, as can be seen, the ITD will be the same for any azimuth angle and its compliment, that is 180° minus the angle of the azimuth. This is as predicted from the previous discussion regarding the "cone of confusion". ILD analysis coupled with pinna effects modeling is required to resolve whether the azimuth is an anterior or posterior angle.

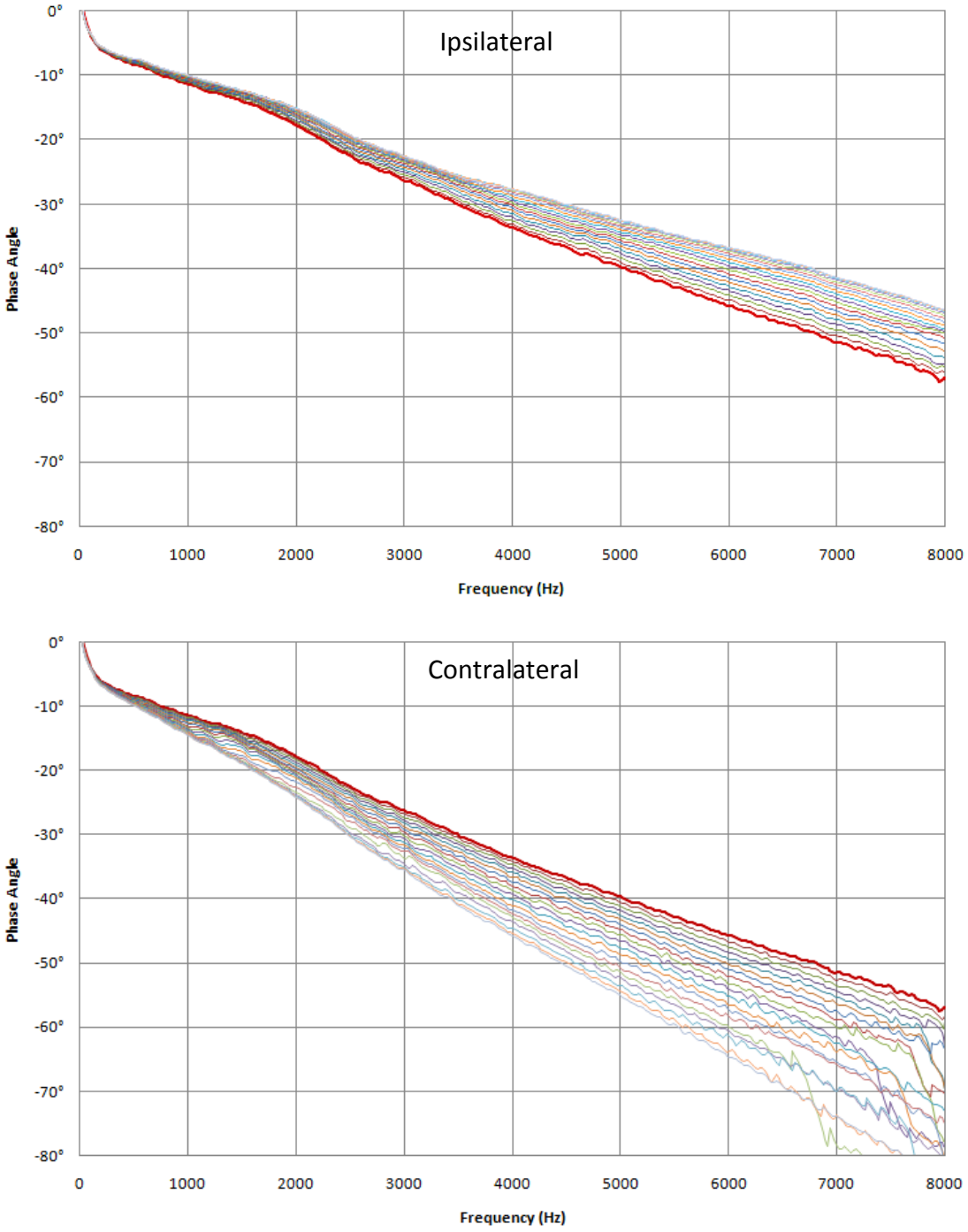

Figure 17. Phase at each ear as azimuth is varied between 0° and 90° (top is the ipsilateral ear and bottom is the contralateral), for normal hearing. In the ipsilateral ear the slope of the phase curve decreases as the azimuth in rotated from 0° to 90°. In the contralateral ear the slope of the phase curve increases as the azimuth in rotated from 0° to 90°. In both cases the heavy red line is the phase of the 0° azimuth signal. One can see then from these plots that the phase differential increases as the azimuth is rotated from 0° to 90°.

The results in Figure 16 compare favorably to those obtained from a research subject in a study by Gardner (2004), which are shown here for comparison in Figure 18. One can observe that the patterns exhibited in the signal at an intermediate point in the current model algorithm appear very similar to those published by Gardner. Note that the frequencies at which the first and second notches (N1 and N2) occur match precisely with those obtained from the normal hearing model. These closely matching plots are taken as validation that the base component of the localization model, the HRTF, is appropriately implemented. These first and second notches are also important cues which aid in sound source localization.

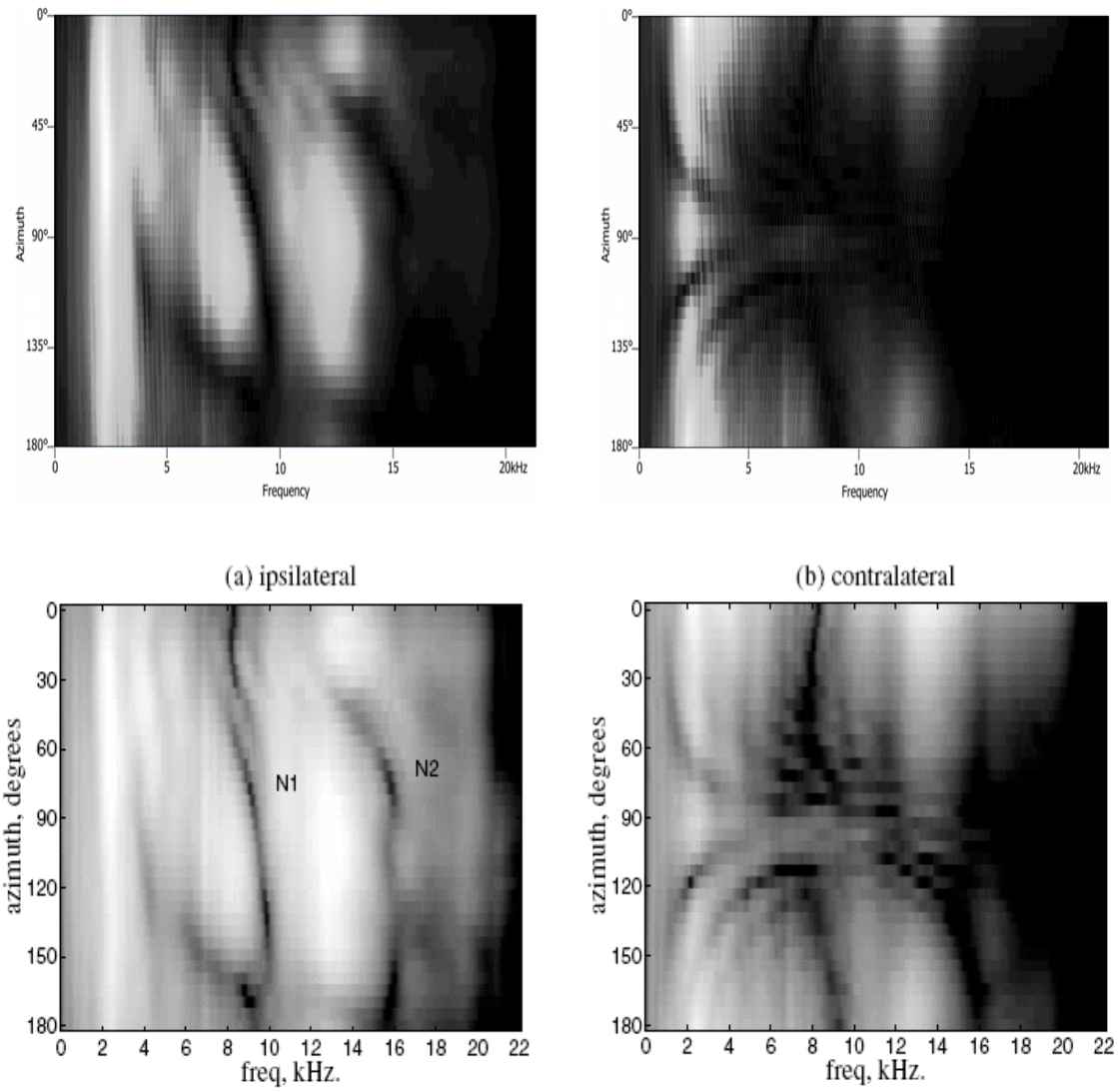

Figure 18. Comparison of HRTFs (magnitude of the response) of the ipsilateral and contralateral ears from the model and Gardner (2004). Note the first and second notches, labeled N1 and N2 in the lower left pane, are closely matched by the model in the upper left pane.

Phase difference of the transfer function for each ear is used to calculate the direction of the sound source in the MatLab model. In Figure 19 the red curve is the calculated phase difference, and the gray curve indicates theoretical values for a spherical head model. Note that the spherical model does not include pinna effects. Any

difference significantly greater than the peak theoretical value results in a calculation error of $\sin(\theta) > 1$.

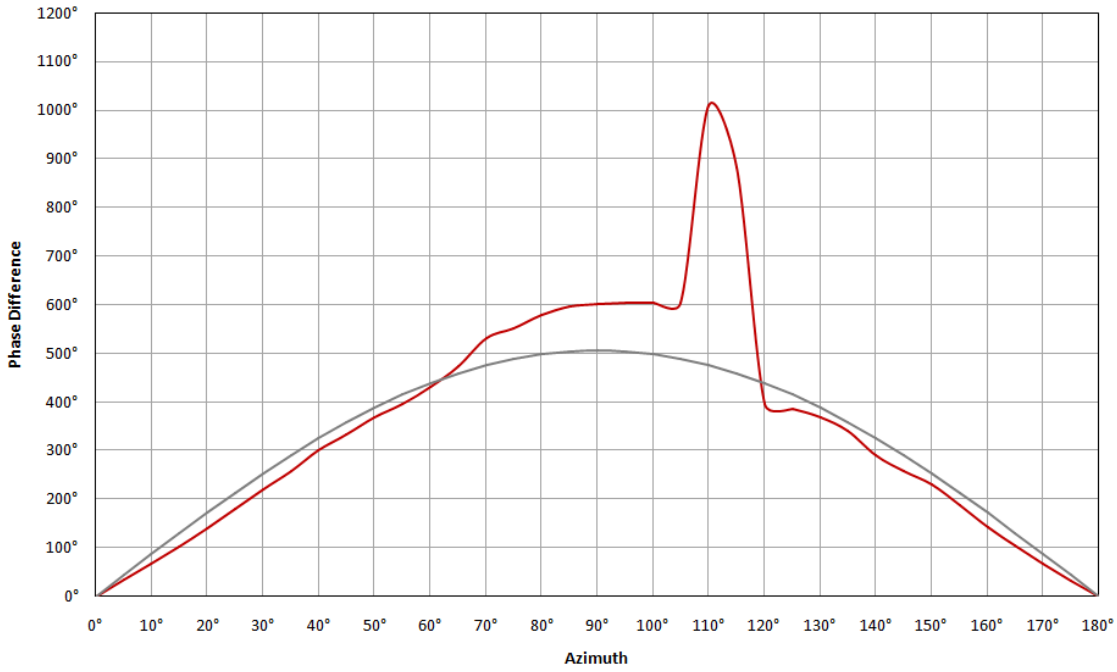

Figure 19. Phase plot showing correlation between azimuth angle and phase angle differential. The red curve is the calculated phase difference, and the gray curve depicts the theoretical values of a spherical head model for phase differential, which are tracked closely at most azimuths.

Early in the development of the model, the magnitude and phase difference elements of the peak spectral component showed a correlation between magnitude trajectory and phase values that resulted in an inability to calculate azimuth. There were two points of discontinuity in the magnitude curve between 65° and 70° and between 110° and 115° that were due to ITD values that were out of bounds, i.e. that resulted in a value greater than unity for the sin of the angle. This was due to sharp transitions in the HRTF caused by pinna effects. Further development of the pinna effects analysis better accounted for the signal characteristics at these azimuths, and thereby eliminated these

errors. Specifically, the pinna model was further refined to more closely approximate the geometry of the structure, so that it more accurately compensated for the excursions in the phase. Thus, the ITD calculation no longer had azimuths which could not be computed. By performing this additional analysis of the phase response, it was found that the curve could be made to better approximate the theoretical curve as shown in Figure 19.

In order to be able to differentiate between signals originating from an anterior location or a posterior location, it was necessary to analyze the relationship between the magnitude and phase component of the source signal. Figure 20 illustrates an example of the magnitude and phase of the signal received at the ipsilateral ear as the signal is varied from 0° to 180°. It can be seen that there are characteristic similarities in the curve for the posterior signal that are not observed in the anterior signals. This is due to "blocking" effects of the pinna on posterior signals. When an analysis was conducted that was based on a filter modeling the pinna, pinna effects were able to be extracted and it was possible to differentiate between anterior and posterior signal sources. Essentially, in this analysis it was found that there exists a relationship between the ratio of the magnitudes of the response at each ear and the phase response of the ipsilateral ear. This characteristic analysis was incorporated into the model in order to differentiate cone of confusion ambiguities.

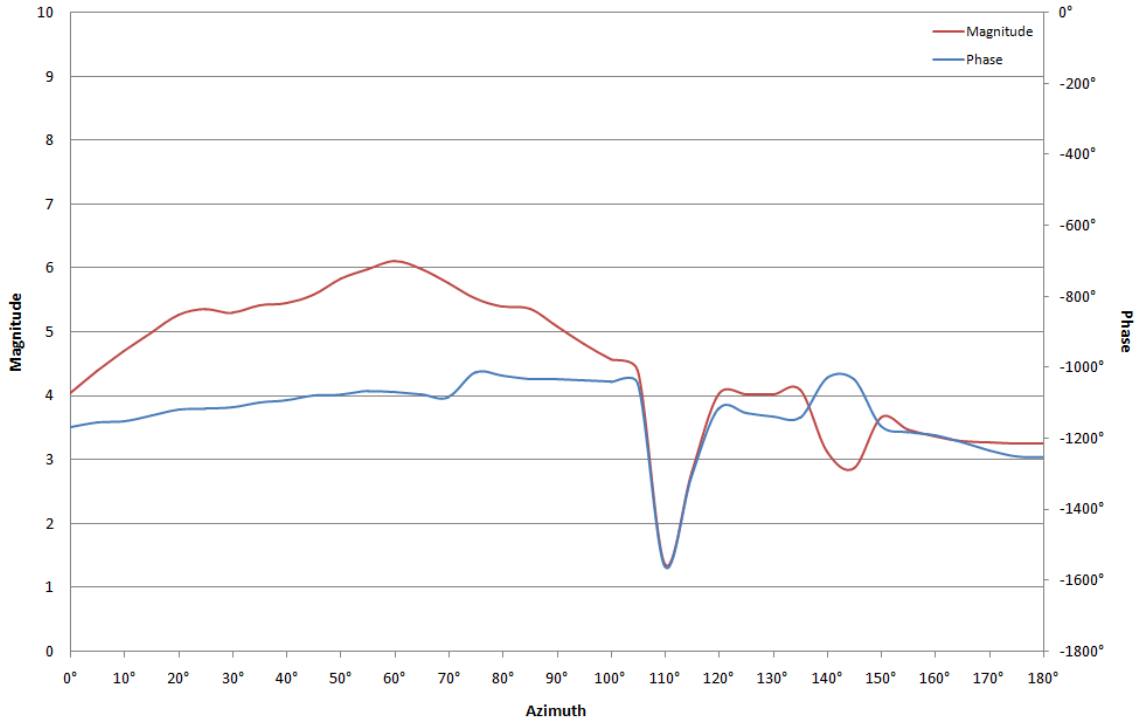

Figure 20. The magnitude of the transfer function (red) is plotted on the left axis. The phase of the transfer function (blue) is plotted on the right axis.

2. Localization performance and discussion

The error of the estimated azimuth compared to the actual azimuth is shown in Figure 21. It can be seen from the plot that due to the angle at which the acoustic wave strikes the pinna, there is still increased error for certain azimuths, but it is much closer to the performance of the normal hearing ear.

Although remaining inadequacies in the pinna effects modeling result in increased error, values between 70° and 95° can now be calculated with an acceptable error. The larger error remaining between 95° and 120° is due to the sharp variations in the transfer function as the azimuth angle passes the point where the pinna is "edge on"; however, adequate results were able to be obtained.

Early results obtained from the normal hearing model did not take into account the finer details of the pinna effects. These earlier results, which were reported by Miller and Matin (2011) had an RMS Error of 4.4°. Refinements in the pinna model reduced this to 4.1°. The implementation of a smoothing filter in order to reduce the granularity of the model output reduced the RMS Error to about 3°, which is within the range of the published data for normal hearing subjects. The error response of the final iteration of the normal hearing model is presented in Figure 21.

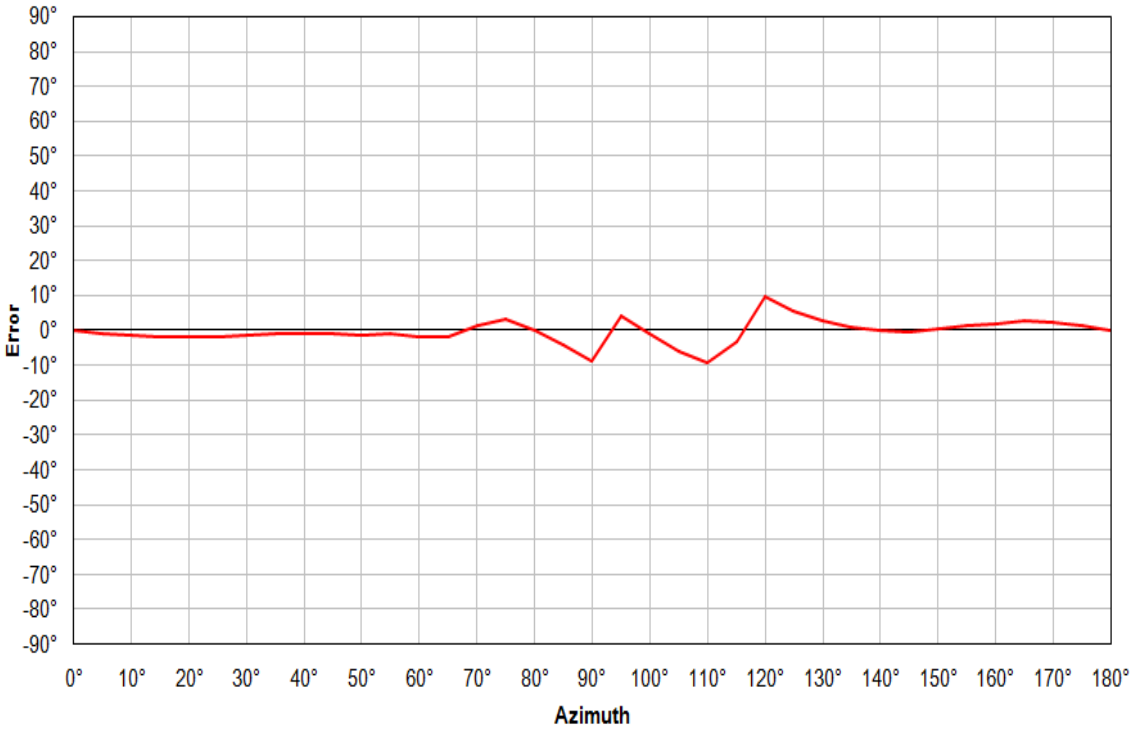

Figure 21. Error plot for the normal hearing model. This error was calculated by subtracting the estimated azimuth from actual azimuth.

The RMS Error of normal hearing subjects is generally accepted to be about 1° for broadband stimuli (Perrott and Saberi, 1990). However, Verschuur *et al.* (2005)

found that normal hearing subjects in their study exhibited localization error in the range of 2° to 3°.

The RMS Error of the completed normal hearing model that is the topic of this dissertation was determined to be 4.1° before a Butterworth filter was applied in order to smooth the results; however, this error is elevated due to the azimuth angles for which there is significant phase excursion related to remaining uncompensated pinna effects. If the two points related to azimuth angles for which pinna effects are not adequately modeled are considered to be outliers and are therefore neglected, the recalculated RMS Error result is 1.7°, which matches well with the published data obtained from normal hearing subjects. Since this model was not intended to exactly match experimental results (which show some variability across studies anyway), but only to provide an acceptable model that could then be used for cochlear implant analysis, this error value seems quite acceptable. It is also expected that further work on the pinna effects analysis and with the ITD analysis to obtain improved ITD coefficient equations might result in an improved error result. It should be noted, however, that since pinna effects do not come into play in the cochlear implant model, improvements in this area would provide no benefit in the cochlear implant localization model performance; thus, these refinements were not pursued in the current work.

Figure 22 illustrates the model localization error in a polar plot superimposed over a top view silhouette of the head. It can be seen in this illustration how the pinna affects the localization ability of a normal hearing person. The model (represented by the red

line) tracks very closely to perfect localization ability (represented by the black line), except for azimuths where the pinna effects are most pronounced.

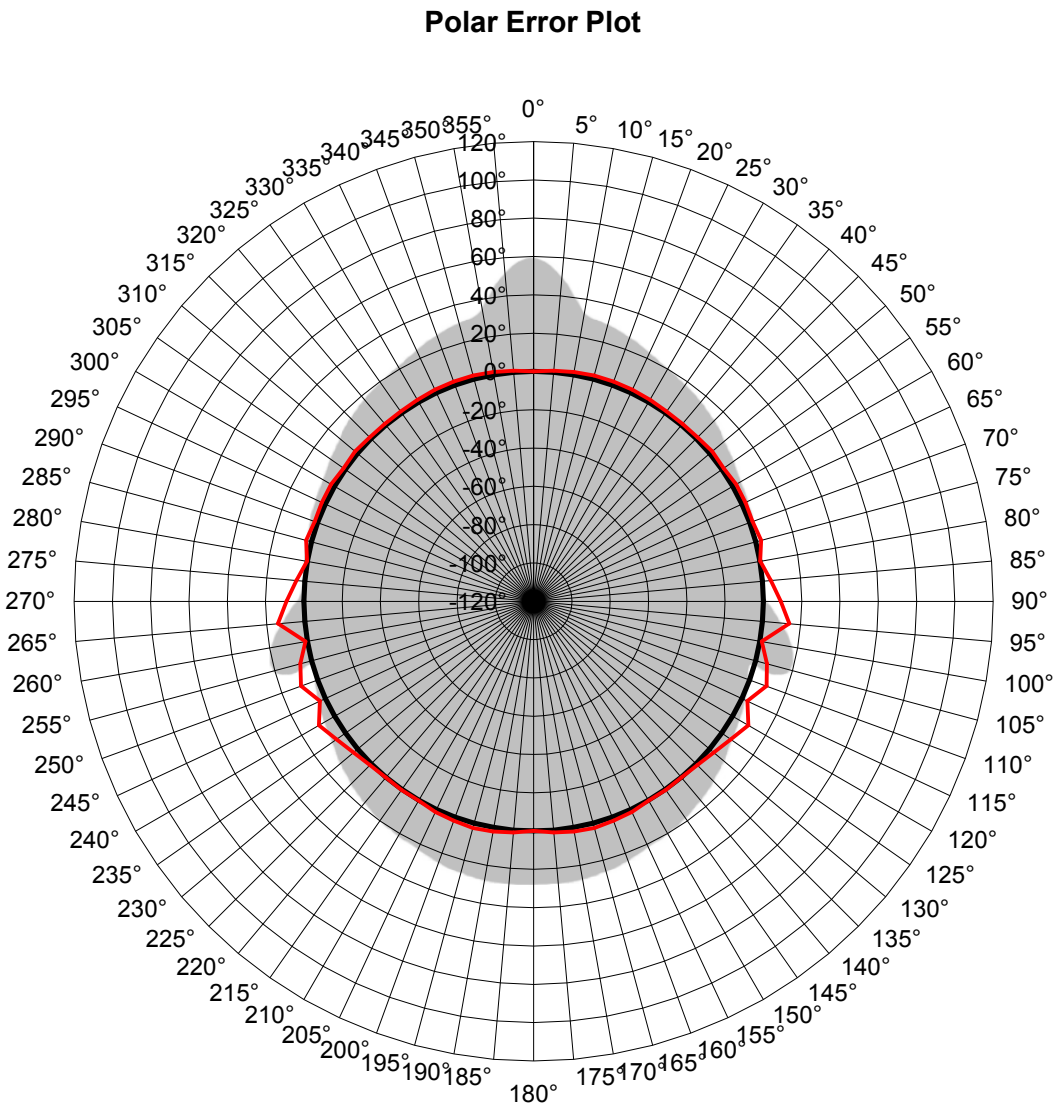

Figure 22. Polar error plot demonstrating the normal hearing model. This plot describes the error magnitude for the normal hearing model superimposed over the silhouette of the head viewed from above. The black circle is the zero-error curve, while the red line corresponds to the magnitude of the model error for normal hearing.

CHAPTER 5

Cochlear Implant Model

1. Results for the cochlear implant model

The same broadband signal, shown in Figure 16, that was used for analysis of the normal hearing model was also applied to the cochlear implant model. The signal analysis performed by the cochlear implant localization algorithm selected the filter bins with the greatest magnitudes, which were bands 7 through 10 for this signal, as defined by the filter structure previously described in Figure 15. When the signal components outside of these four bands are removed, the remaining components that the localization model is left to work with result in the signal shown as a magnitude plot in Figure 23.

It is evident from the comparison of these two signals that the localization algorithm for the cochlear implant condition has a much reduced set of information with which perform the sound source localization task compared to that of the normal ear. In addition, due to filtering of the signal, spectral characteristics are modified at the spectral boundaries of the filter. These changes in the signal will result in a greater difficulty in localizing the sound source, and hence produce increased error results.

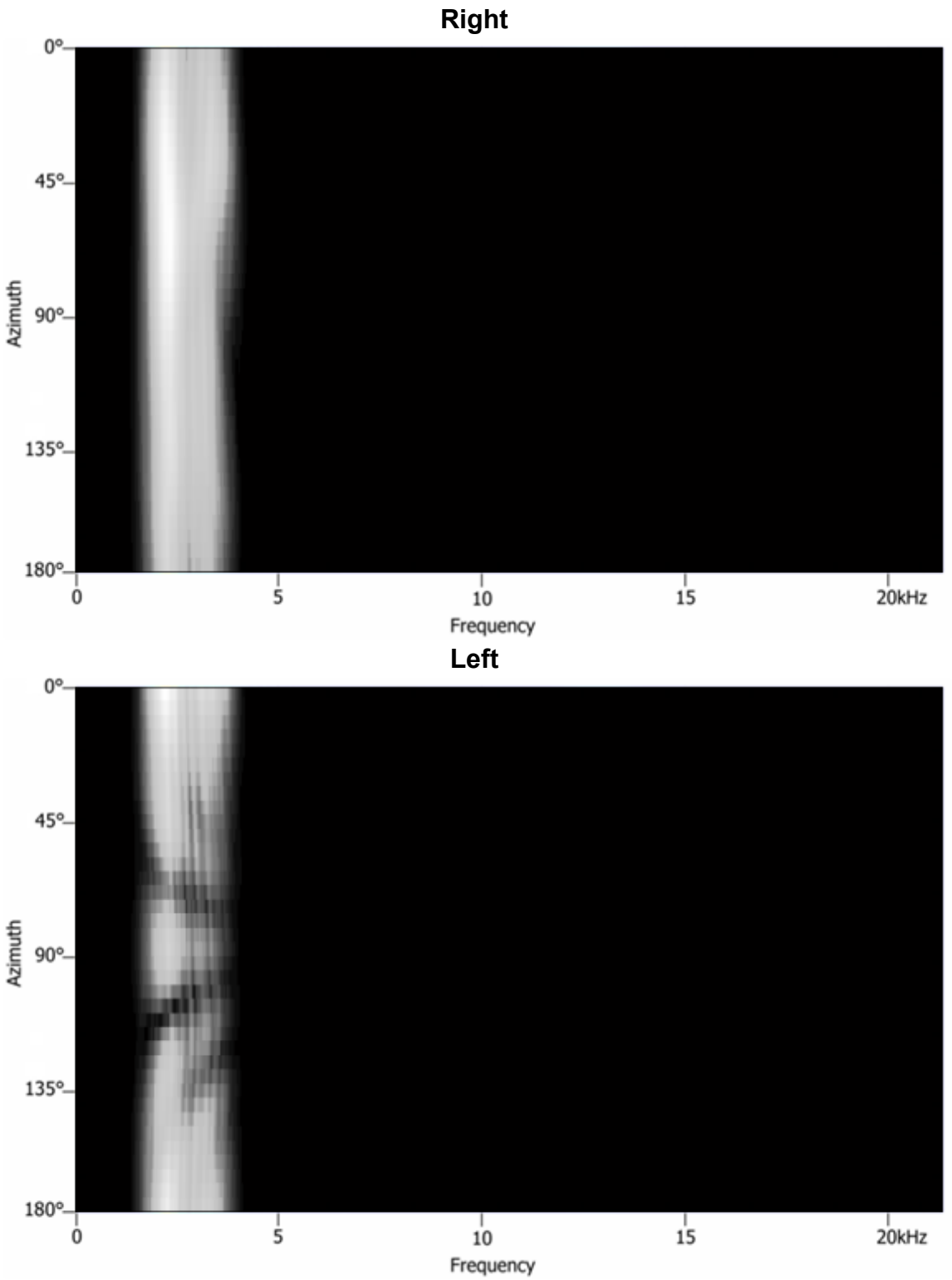

Figure 23. Signal magnitude obtained at each ear as azimuth is varied between 0° and 180° (right is the ipsilateral ear and left is the contralateral). This is the same signal that was used in the normal hearing plots in Figure 16, but following processing by the cochlear implant.

Pinna and head shadow effects can be observed by examining the magnitude of the Fourier transformed signals. Figure 24 shows a comparison of the normal hearing response magnitude versus that of the cochlear implant model. In the ipsilateral ear of the normal model, pinna effects can clearly be seen represented by sharp dips in the response as the signal azimuth moves to the anterior of the pinna. In contrast, the cochlear implant model shows no effect of the pinna because the signal is picked up by a microphone located above the pinna.

The head shadow effect, on the other hand, is present with both models. It can be seen in the plot that the contralateral ear has nearly identical responses for the normal and cochlear implant models. This is intuitively obvious since the head blocks the signal pathway to the contralateral ear in a similar fashion for either condition.

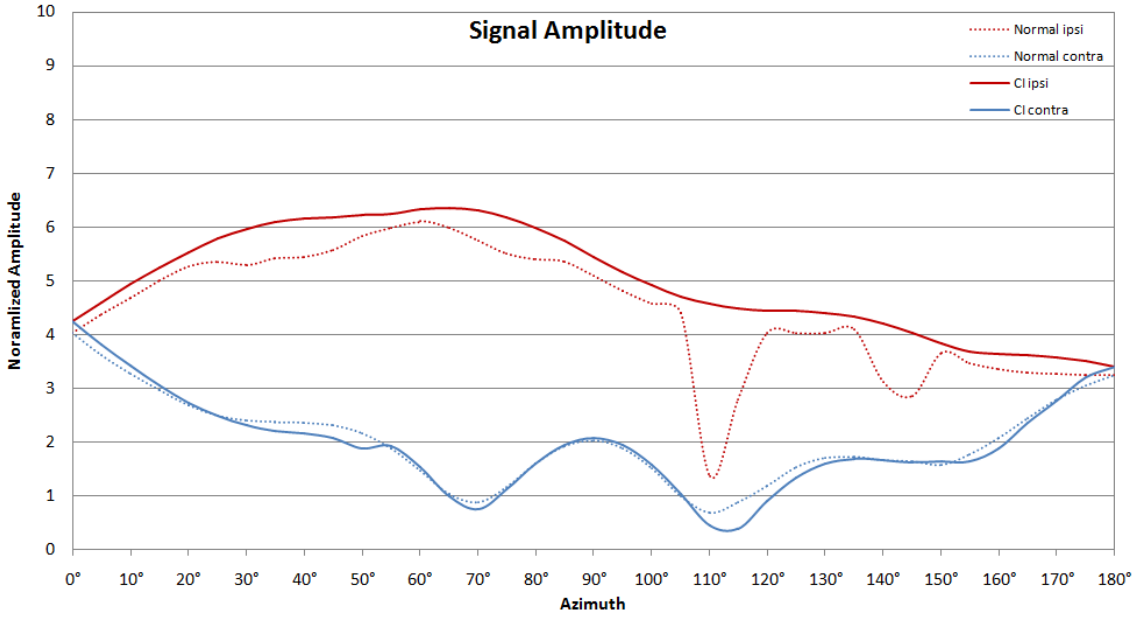

Figure 24. Comparison of normal and cochlear implant signal amplitudes as azimuth is varied from 0° to 180° for the ipsilateral and contralateral ears. One can clearly see the pinna and head shadow effects.

Figure 25 shows the phase response for the ipsilateral and contralateral ears of a cochlear implant user as generated by the model. In the same plot for the normal hearing model, which was shown in Figure 19, there was a natural progression of the response as azimuth was incremented, but that is not seen here. In the normal hearing ear, the change in azimuth causes an ordered progression of the phase angle with increasing azimuth angle. Specifically, the slope of the phase angle curve decreases with increasing azimuth in the ipsilateral ear, while the slope of the phase angle curve increases with increasing azimuth for the contralateral ear.

In contrast, it can be seen in the phase plots in Figure 25 that the cochlear implant model does not have a constant rate of change in phase angle in the ipsilateral ear, and the contralateral ear does not even always show an increase in the slope of the phase angle curve. Some of the azimuths have steeper slopes in the phase angles than that for 0° azimuth. These much less orderly characteristics of the set of phase angle curves would lead to the much poorer localization performance as experienced by cochlear implant users.

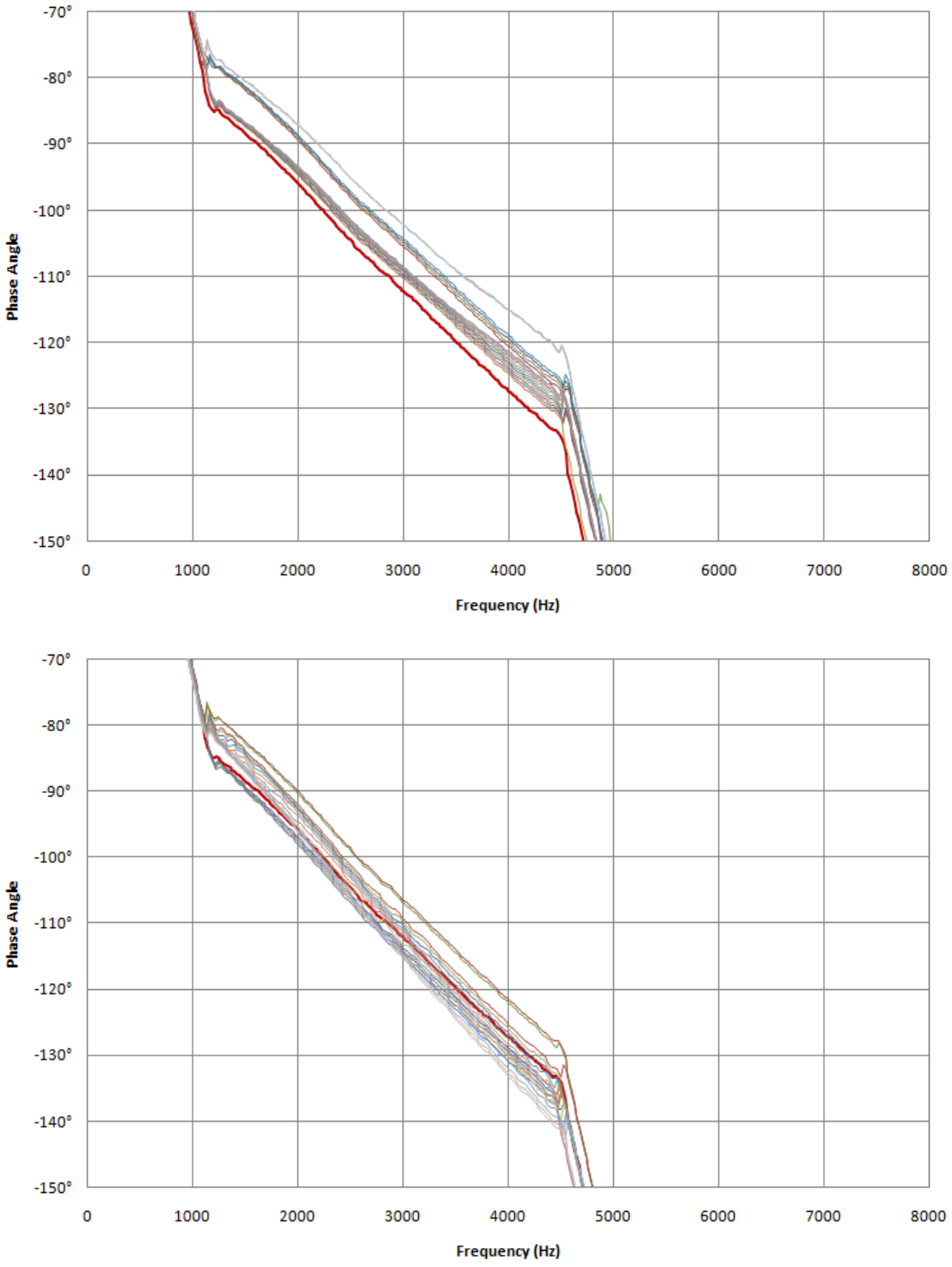

Figure 25. Phase responses for the ipsilateral ear (top) and the contralateral ear (bottom), as modeled for a cochlear implant.

This leads to greater variability in the phase differential curve. The difference in the phase differential compared to normal hearing can be seen in the plot below (Figure 26). It is evident from this plot that the cochlear implant phase differential varies much more from the expected value, the gray curve, than does that of the normal hearing subjects.

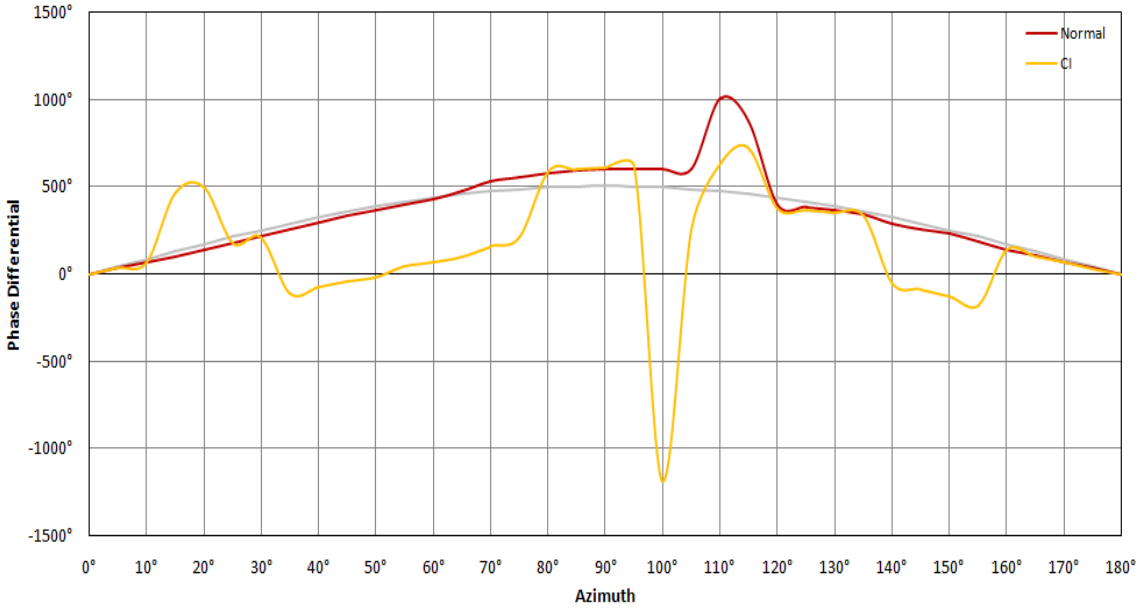

Figure 26. Phase differential for CI (yellow) as compared to the normal hearing model (red) and the ideal curve (gray).

2. Localization performance and discussion

As would be expected from the phase differential plot, Figure 27 illustrates that localization error is considerably greater for cochlear implant users than for normal hearing subjects (which was shown in Figure 21). Much of this error appears to be a result of the missing pinna effects that aid in the determination of whether the signal is originating from an anterior location or a posterior one. However, it appears that other

factors come into play as well, since the error is pronounced in azimuths that are less affected by pinna effects in normal hearing subjects. This can be explained by spectral and quantization distortions related to the cochlear implant signal processing.

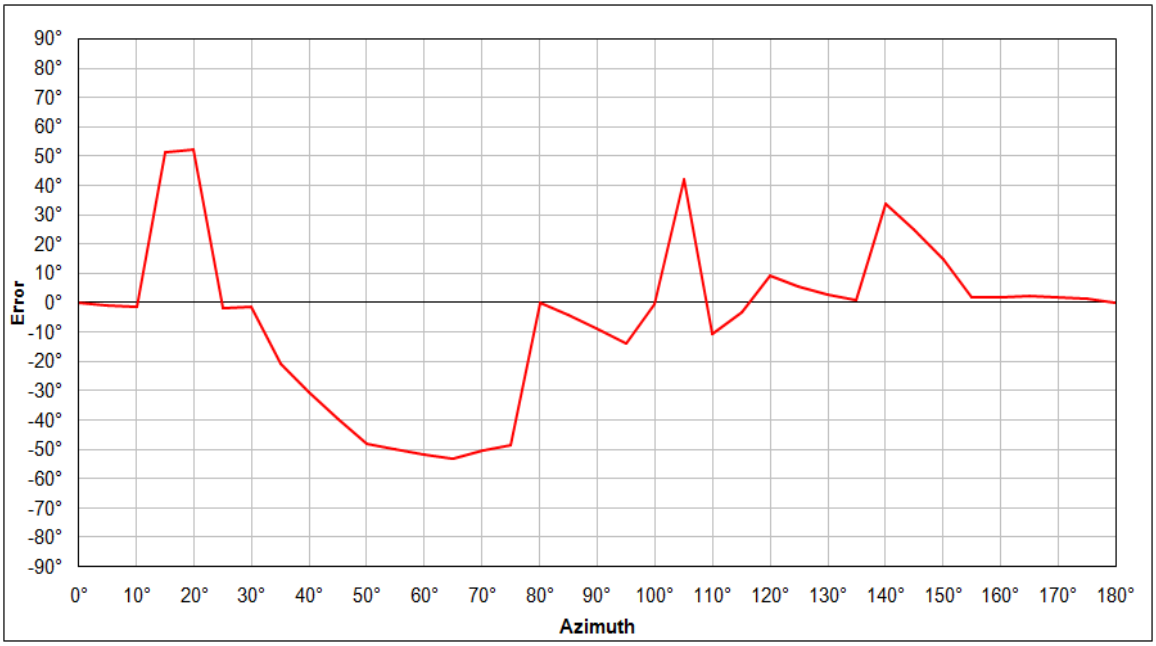

Figure 27. Error plot for the cochlear implant model. This error was calculated by subtracting the estimated azimuth, as detected by the model, from the actual azimuth.

Figure 28 attempts to provide a more visual representation of the localization error by overlaying the error plots for normal hearing and cochlear implants on a polar plot with a top view of a silhouette of the head. In this figure the dark black line represents "zero error" and the red line is the normal hearing localization error as determined through the model. The yellow line represents the cochlear implant localization error as determined through the model. In this polar plot a moving average filter was applied to the data in order to better represent a continuous error curve.

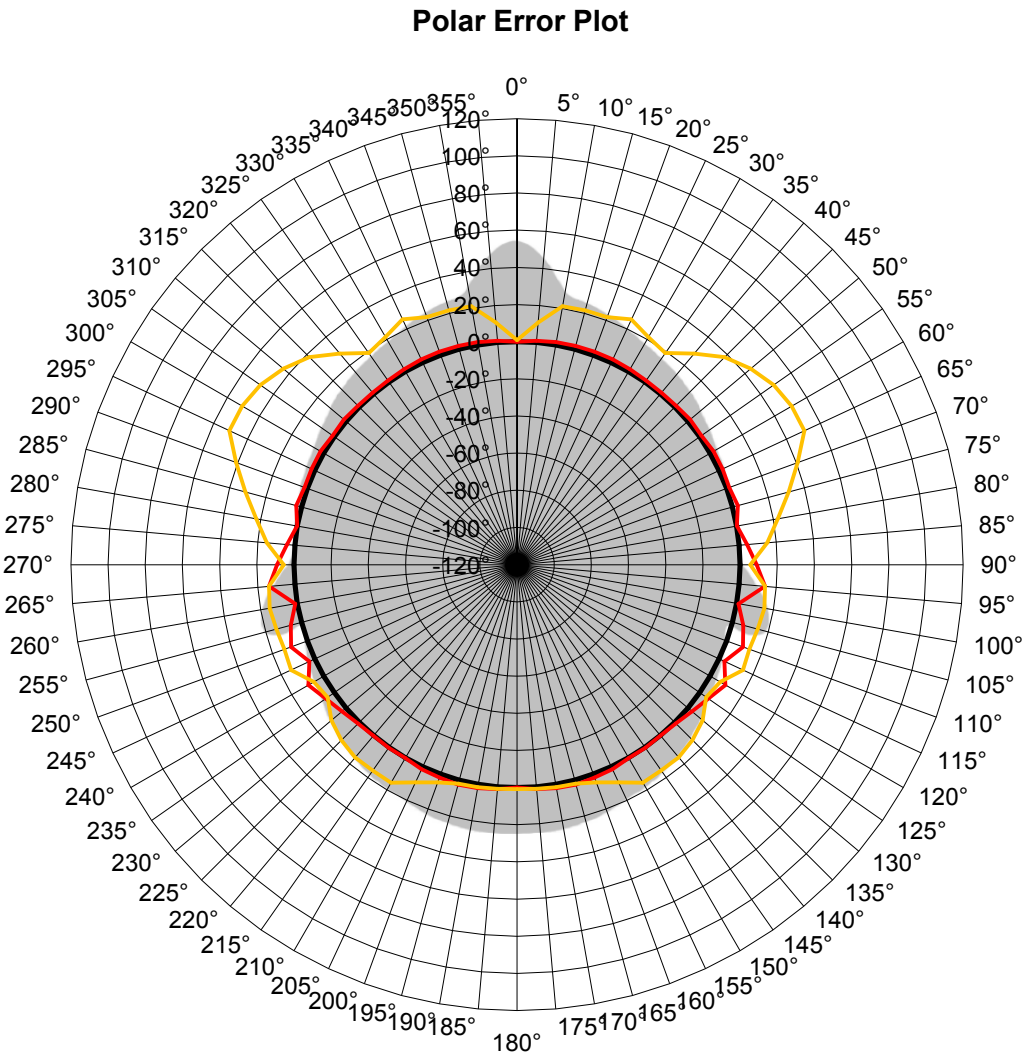

Figure 28. Polar error plot comparing the normal hearing model to the cochlear implant hearing model. These error curves describe the error magnitude for each model super-imposed over the silhouette of the head viewed from above. The black circle is the zero-error curve, the red line corresponds to the model error for normal hearing, and the yellow line corresponds to cochlear implant localization error as projected by the model.

Error data was obtained from published localization studies in order to evaluate whether the cochlear implant model's performance was representative of the typical performance of cochlear implant subjects. Verschuur *et al.* (2005) studied localization ability in the horizontal plane of 20 adult bilateral cochlear implant users. The subjects'

cochlear implants were all Nucleus 24 devices. Testing was performed at between 3 and 9 months after initial activation of the second implant so that the subjects had time to learn to use the new binaural cues.[9] There were five different stimuli used (speech, tones, noise, transients, and reverberant speech), presented through an 11-loudspeaker array in ±5 dB steps around 60 dB SPL. Analysis of variance with post-hoc t-tests determined there was a mean localization error with bilateral listening of 24°, which was significantly better than with unilateral listening conditions, as shown in Figure 29.

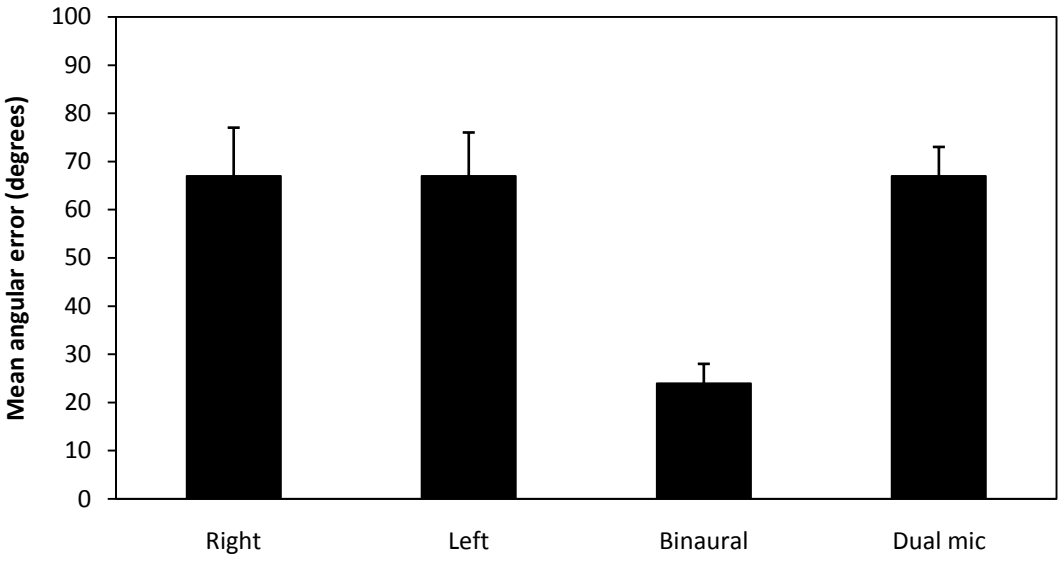

Figure 29. Mean angular error on a localization task as a function of listening condition: unilateral use of each cochlear implant, bilateral cochlear implants, and unilateral condition with a "dual" (port) microphone. A smaller bar indicates better performance. (Recreated from Vershuur *et al*., 2005)

In this study, it was noted that the performance of normal controls, as assessed previously by the authors, averaged 2° to 3° localization error. The authors hypothesized

[9] Cochlear implant users typically show improved performance over a period of 3 to 12 months following implantation, a process generally referred to as "acclimatization".

that the cochlear implant users' poorer performance was due to the absence of temporal fine-structure cues, limitations associated with absolute level judgments due to amplitude quantization in the CIs, or inability to compare the amplitude spectrum between the ears limiting ILD perception. The type of auditory stimulus had no significant effect on performance.

Other published studies showed similar values for localization error in cochlear implant users. Litovsky *et al*. (2006) tested 13 bilateral cochlear implant subjects for localization performance by presenting an audio signal through one of two speakers placed equidistant from the median plane and determined the minimum angle offset from 0° azimuth that the subject could correctly identify the source. The mean minimum angle for the group was 20°.

Grantham *et al*. (2007) examined 22 adult bilateral cochlear implant users' localization ability for 200 msec noise bursts or speech samples presented at 70 dB SPL (roved ± 10 dB) from a 43-loudspeaker horizontal array ranging from 90° to 270° azimuth, with 17 speakers active, in an anechoic chamber. Results indicated that bilateral listening performances were better than the best of the two unilateral ear performances. The mean adjusted constant error for bilateral listening was 22.8°, while for unilateral listening it was 47.9° (or just above chance).

Neuman *et al*.(2007) tested 8 bilateral cochlear implant subjects using an array of nine loudspeakers placed in an arc evenly spaced from -90° to 90°. The signal was randomly roved among all loudspeakers while the subject reported which loudspeaker

they believed was the source. RMS Error was calculated for a total of 36 tests for each of 8 subjects. The RMS Error from this study are shown in Figure 30. This localization error assessment technique very closely approximated the error determination methods used for evaluating the model developed in this dissertation. The RMS Error result reported in the Neuman *et al*. study was 29°.

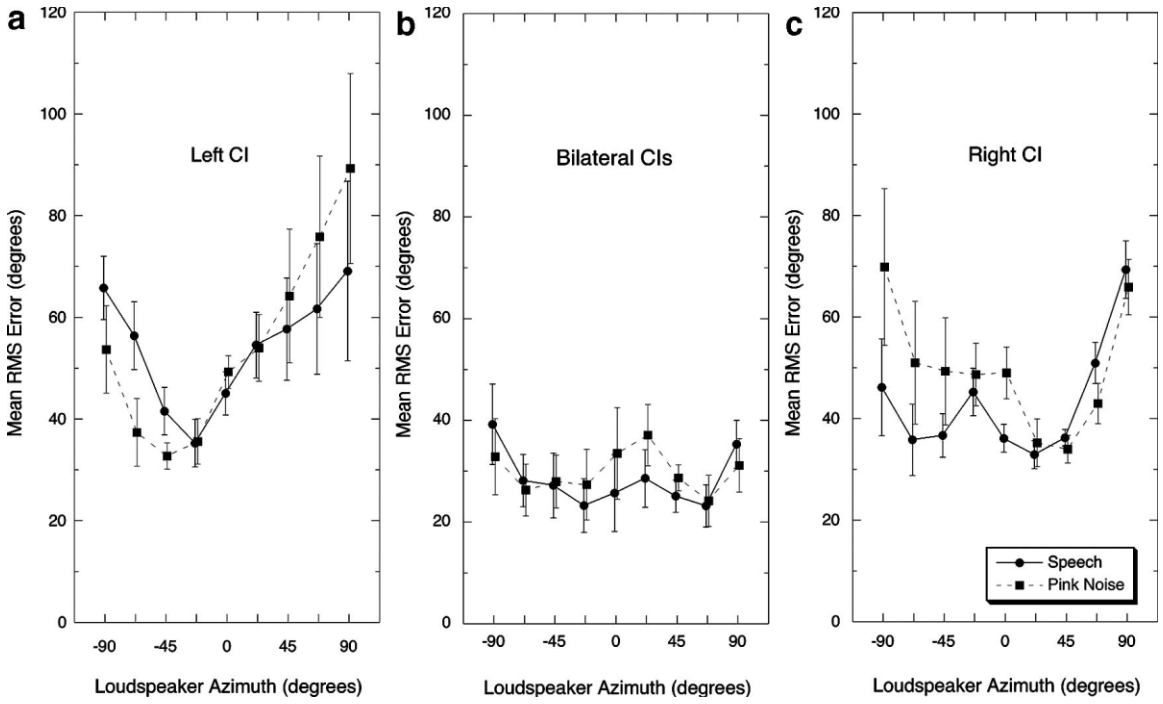

Figure 30. Localization error results for the bilateral testing conducted by Neuman *et al.* (2007).

Combining the outcomes reported in these published studies on bilateral cochlear implant users results in a range of mean localization errors of 20° to 29°. By comparison the RMS Error of 27° obtained with the cochlear implant MatLab model developed in this study fits well within the range found in the published literature.

CHAPTER 6

Summary and Future Work

1. Summary

In this work models were developed for simulating the localization ability of normal hearing subjects and bilateral cochlear implant users. These models were validated against published data for both groups and found to give similar localization error for each group to that shown in the literature.

Much refinement of the models were done in order to approximate the performance of the biological system in both the normal hearing and cochlear implant conditions. It was found that by determining the sign of the phase differential, the model could determine the side of the head that the sound source signal was located on. Pinna effects analysis and head shadow coefficient equations were developed that resulted in the model's ability to more accurately resolve the angle to the sound source. Implementation of these additional features in the model not only improved the accuracy, but also removed the inability to resolve ITD values for certain azimuths near 90° and 270°. Thus it provided a model capable of localization of sound sources for the full 0° to 360° range.

Only the ACE cochlear implant signal processing algorithm was approximated in the model devised for this dissertation, although there are other signal processing algorithms used in cochlear implants. The ACE algorithm was selected because this is the most prevalent method currently employed in devices in use today. However, since it was built into the model as a function, this algorithm could be easily replaced or modified to reflect other signal processing algorithms that are now in use. In addition, using the model developed here, newly proposed algorithms could be easily tested for an estimate of signal source localization performance without first spending considerable time and resources developing hardware and software. Also, all new processing sysetms would need to be put through the exhaustive testing regimens that are required before being placed in a human subject for testing.

While the pinna effects and head shadow coefficient used in this model could undoubtedly be further improved, the focus of this research was to develop a model that reasonably matched real world performance, so that it could be used to evaluate cochlear implant sound processor algorithms. It is also certain that the cochlear implant signal processing algorithm could more exactly follow the performance of commercially marketed devices. However, since the RMS Error results achieved with the models developed in this work were similar for normal hearing subjects and for bilateral cochlear implant subjects to those published in the literature for each group, the goal of this research was successfully met.

As Blommer and Wakefield (1997) noted, a pole-zero model for HRTF will not give an exact representation of the HRTF. However, looking at the RMS Error results

presented in Table 1, it appears that the pole-zero HRTF can still provide an adequate basis for the localization model. Also, although the normal hearing model error was slightly greater than the published figures, it is believed that this was primarily due to an imperfect pinna effects model function. Since pinna effects play an insignificant role when evaluating cochlear implants, it is thought that the source of this elevated error was not carried over into the cochlear implant localization model.

Table 1. RMS Error of model compared to published data.

	Model	Published test subject data
Normal Hearing	4°	2° to 3° [a]
Bilateral cochlear implants	27°	20° to 29° [b]

[a] from Verschuur *et al.* (2005).
[b] combined from Verschuur *et al.* (2005), Litovsky *et al*. (2006), Grantham *et al.* (2007) and Neuman *et al*. (2007).

2. Future work

There is, of course, still much work that could be conducted in this area. The following is a list of some of the most obvious and interesting subjects where this research could continue:

- The MatLab modeling work could be continued to include improvement of the model through refinement of the pinna effects transfer function. This could lead to more accurately matching the performance of the model to that of a normal hearing person. This could also be better validated to experimental results

through comparison of the model to measured results by azimuth, rather than the aggregate error as was found in the published data by Perrott and Saberi, (1990) and Verschuur *et al.* (2005).

- An area that was not given consideration in the model presented in this dissertation is refinement of the signal processing algorithm representing echoes and delays associated with the microphone placement in cochlear implant external processors. Since an assumption was made that this would not have nearly as significant an impact on performance as the signal processing of the implant itself, no effort was exerted in this area. While this assumption is still considered to be valid, addressing this aspect of the modeling of the cochlear implant would be expected to provide a slightly closer match to the signal that eventually is processed for sound source localization. Incorporation of this feature would also provide the ability to assess new microphone placement schemes, and whether they have any impact on localization performance.
- While sound source localization performance of the model did reasonably match that of cochlear implant subjects as reported in the literature, additional work could be conducted in order to include more detailed modeling of the cochlear implant signal processing. Through more exactly following the commercial algorithm, which would require obtaining proprietary information from the manufacturer, it is assumed that the performance could be more closely matched. In order to assess whether there is a better match of the performance than that shown in this work, it would also be necessary to obtain a deeper analysis of the subject performance data, so that a comparison by azimuth could be conducted.

- Finally, an area that would be of significant interest would be to develop additional models for other commonly used cochlear implant processors and compare the models' performance to published data on these types of sound processors. It would be of great interest to see if the close correlation in localization error seen in the current model continues with other cochlear implant signal processing algorithms.

  This would necessarily be a larger research project than this dissertation because proprietary information regarding the signal processing algorithms would be required, since only the CIS algorithm has specifics published in any detail. It would also be necessary to conduct cochlear implant sound source localization studies where the population was controlled for signal processing type, in order to obtain the required data for comparison.

3. Conclusion

The close correlation between published data on localization abilities of cochlear implant users and the modeled localization performance results from the current study suggest that their poor performance is primarily due to the combination of differences in the HRTF and degradation of the cues by the signal processing of the implant. The HRTF differences are essentially reduced pinna effects and thus the loss of the additional auditory cues that are created when presented with other than a monotonic acoustic signal. However, the loss of the full set of auditory cues caused by the signal processing algorithm employed by the cochlear implant is likely to play a larger role with most signals presented.

In conclusion, this sound source localization model is deemed suitable as a tool for evaluating cochlear implant signal processing algorithms for localization performance. It is believed that this model could become an important element in the development of new cochlear implant signal processing algorithms, if provided to researchers and engineers working in this area.

Bibliography

Adams, N. H. and Wakefield, G. H. (2009). State-space models of head-related transfer functions for virtual auditory scene synthesis. *J. Acoust. Soc. Am.,* 125(6): 3894-3902.

Aitkin, L. M. and Martin, R. L. (1987). The representation of stimulus azimuth by high best-frequency azimuth-selective neurons in the central nucleus of the inferior colliculus of the cat. *J. Neurophysiol.,* 57(4): 1185-1200.

Aitkin, L. M. and Martin, R. L. (1990). Neurons in the inferior colliculus of cats sensitive to sound-source elevation. *Hear. Res.,* 50: 97-106.

Algazi, V. R., Duda, R. O., Morrison, R. P., and Thompson, D. M. (2001). Structural composition and decomposition of HRTFs. *2001 IEEE Workshop on the Applications of Signal Processing to Audio and Acoustics,* (0-7803-7126-7): 103-106.

Algazi, V. R., Duda, R. O., Duraiswami, R., Gumerov, N. A., and Tang, Z. (2002). Approximating the head-related transfer function using simple geometric models of the head and torso. *J. Acoust. Soc. Am.,* 112 (5): 2053-2064.

Armstrong, M., Pegg, P., James, C., and Blamey, P. (1997). Speech perception in noise with cochlear implant and hearing aid. *American Journal of Otology*, 18: S140-S141.

Asano, F., Suzuki, Y., and Sone, T. (1990). Role of spectral cues in median plane localization. *J. Acoust. Soc. Am.,* 88(1): 159-168.

Bai M. R. and Tsao T. C. (2006). Numerical Modeling of Head-Related Transfer Functions Using the Boundary Source Representation. *J. Vib. Acoust.,* 128: 594-603.

Balkany, T., Boggess, W., and Dinner, B. (1988). Binaural cochlear implantation: comparison of 3M/House and Nucleus 22 devices with evidence of sensory integration. *Laryngoscope*, 98(10): 1040-1043.

Beijen J. W., Snik A. F., and Mylanus E. A. (2007). Sound localization ability of young children with bilateral cochlear implants. *Otol. Neurotol*., 28(4): 479-485.

Birchfield, S. T. and Gangishetty R. (2005). Acoustic localization by interaural level difference. In: *IEEE International Conference on Acoustics, Speech, and Signal Processing (ICASSP)* Philadelphia, Pennsylvania, March 2005, iv-1109.

Blamey, P. J., Dooley, G. J., Prisi, E. S., and Clark, G. M. (1996). Pitch comparisons of acoustically and electrically evoked auditory sensations. *Hearing Research*, 99: 139-150.

Blauert, J. (1970). Sound localization in the median plane (Frequency function of sound localization in median plane measured psychoacoustically at both ears with narrow band signals). *Acustica*, 22(4), 205-213.

Blauert, J. (1997). Spatial Hearing (Revised Edition): The Psychophysics of Human Sound Localization. MIT Press, Cambridge, MA.

Blommer, M. A. and Wakefield, G. H. (1992). Investigation of phase distortion in the synthesis of head related transfer functions. *J. Acoust. Soc. Am*., 92(4): 2297-2297.

Blommer, M. A. and Wakefield, G. H. (1994). On the design of pole-zero approximations using a logarithmic error measure. *Signal Processing, IEEE Transactions* 42(11): 3245-3248.

Blommer, M. A. and Wakefield, G. H. (1997). Pole-zero approximations for head-related transfer functions using a logarithmic error criterion. *Speech and Audio Processing, IEEE Transactions*, 5(3): 278-287.

Bronkhurst, A. W. and Plomp, R. (1988). The effect of head-induced interaural time and level differences on speech intelligibility in noise. *J. Acoust. Soc. Am.*, 86: 1374-1383.

Bronkhurst, A. W. and Plomp, R. (1990). A clinical test for the assessment of binaural speech perception in noise. *Audiology*, 29: 275-285.

Brown C. P. and Duda R. O. (1997). An efficient HRTF model for 3-D sound. *IEEE Workshop on Applications of Signal Processing to Audio and Acoustics*, Oct 1997: 4-7.

Brown, C. P. and Duda, R. O. (1998). A structural model for binaural sound synthesis. *Speech and Audio Processing, IEEE Transactions*, 6(5): 476-488.

Brown K. D. and Balkany T. J. (2007). Benefits of bilateral cochlear implantation: a review. *Curr. Opin. Otolaryngol. Head. Neck. Surg*., 15(5): 215-318.

Buss, E., Pillsbury, H., Buchman, C., *et al*. (2008). Multicenter U.S. Bilateral Med-El Cochlear Implantation Study: Speech perception over the first year of use. *Ear Hear*, 29(1): 20-32.

Butler, R. A. and Belendiuk, K. (1977). Spectral cues utilized in the localization of sound in the median sagittal plane. *J. Acoust. Soc. Am.,* 61(5): 1264-1269.

Casseday, J. H. and Neff, W. D. (1973). Localization of pure tones. *J. Acoust. Soc. Am*., 54(2): 365-372.

Chanda P. S. and Park S. J. (2005). Low order modeling for multiple moving sound synthesis using head-related transfer functions' principal basis vectors. *Int. Joint Conf. on Neural Networks 2005 (IJCNN05)*, Montreal, Canada.

Chase, S. M. and Young, E. D. (2006). Spike-timing codes enhance the representation of multiple simultaneous sound-localization cues in the inferior colliculus. *J. Neurosci.*, 26(15): 3889-3898.

Cheng, C. I. and Wakefield, G. H. (1999). Spatial frequency response surfaces: an alternative visualization tool for head-related transfer functions (HRTFs). In: *Proc. IEEE Intl Conf Acoustics, Speech and Signal Process*, 2: 961-964.

Cheung N. M., Trautmann, S., Horner, A. (1998). Head-related transfer function modeling in 3-D sound systems with genetic algorithms. In: *Proc. IEEE Intl Conf Acoustics, Speech and Signal Process*, Vol 6: 3529-3532.

Chung W., Carlile S., and Leong P. (2000). A performance adequate computational model for auditory localization. *J. Acoust. Soc. Am.,* 107(1): 432-445.

Das, S. and Buchman, C. (2005). Bilateral cochlear implantation: current concepts. *Current Opin. in Otolaryngol. Head Neck Surg.*, 13: 290-293.

Donoho, D. L. (1995). Denoising by Soft-thresholding. *IEEE Trans. Inf. Theory*, 41: 613-627.

Donoho, D. L. and Johnstone, I. M. (1995). Adapting to Unknown Smoothness via Wavelet Shrinkage, *J. Am. Statist. Ass*., 90: 1200-1224.

Duda, R. O. (2000). An introduction to human spatial hearing. *http://phosphor.cipic.ucdavis.edu*.

Dunn C., Tyler R., Oakley S., Gantz, B. J., Noble, W. (2008). Comparison of speech recognition and localization performance in bilateral and unilateral cochlear implant users matched on duration of deafness and age at implantation. *Ear Hear*, 29(3): 352-359.

Durant, E. A., and Wakefield, G. H. (2002). Efficient model fitting using a genetic algorithm: pole-zero approximations of HRTFs, *Speech and Audio Processing, IEEE Transactions*, 10(1): 18-27.

Durlach, N. I. and Colburn, H. S. (1978). Binaural phenomena. *Handbook of perception*, 4, 365-466.

Faller K. J. , Barreto A., Rishe N. (2009) A new inverse processing approach to the modeling of head-related transfer functions for audio spatialization. *Inverse Problems in Science and Engineering*, 17(1):51-63.

Gardner W. G. and Martin K. D. (1995) HRTF measurements of a KEMAR. *J. Acoust. Soc. Am.*, 97(6): 3907-3908.

Gardner B. (2004) Spatial Audio Reproduction: Towards individualized binaural sound. *From: Wave Arts presentation*. Wave Arts, Inc., Arlington MA.

Gathercole, C. and Mantooth, H. A. (2001). Pole-zero localization: a behavioral modeling approach. In: *Proc of the Fifth IEEE International Workshop on Behavioral Modeling and Simulation*, p. 59-65.

Gelfand, S. A. (2009). Essentials of audiology. Thieme, New York.

Grantham, D. W., Willhite, J. A., Frampton, K. D., and Ashmead, D. H. (2005). Reduced order modeling of head related impulse responses for virtual acoustic displays. *J. Acoust. Soc. Am.*, 117(5): 3116-3125.

Grantham, D., Ashmead, D., Rickets, T., Labadie, R. F., Haynes, D. S. (2007). Horizontal-plane localization of noise and speech signals by postlingually deafened adults fitted with bilateral cochlear implants. *Ear Hear.*, 28(4): 524-541.

Green Jr., J. D., Mills, D. M., Bell, B. A., Luxford, W. M., Tonokawa, L. L. (1992). Binaural cochlear implants. *Amer. J. Otology*, 13(6): 502-506.

Gumerov N. A., O'Donovan A. E., Duraiswami R. and Zotkin D. N. (2010) Computation of the head-related transfer function via the fast multipole accelerated boundary element method and its spherical harmonic representation. *J. Acoust. Soc. Am.*, 127 (1):370-386.

Hacihabiboglu, H. (2002). Interpolation of low-order HRTF filters using a zero displacement measure. *EAA Convention, Proc. Forum Acusticum Sevilla* (CD-ROM), Sevilla, Spain.

Hacihabiboglu, H., Gunel, B., and Murtagh, F. (2002). Wavelet-based spectral smoothing for head related transfer function filter design. *Proc. of the AES 22nd International Conference on Virtual, Synthetic and Entertainment Audio*, Espoo, Finland.

Haneda, Y., Makino, S., Kaneda, Y., and Kitawaki, N. (1999). Common-acoustical-pole and zero modeling of head-related transfer functions. *Speech and Audio Processing, IEEE Transactions*, 7(2): 188-196.

Hebrank, J. and Wright, D. (1974). Spectral cues used in the localization of sound sources on the median plane. *J. Acoust. Soc. Am*., 56(6): 1829-1834.

Helms, J,, Muller, J,, and Schon, F. (2004). Bilateral cochlear implantation, experiences and perspectives. *Otolaryngol. Pol*. 58(1): 51-52.

Hochberg, I., Boothroyd, A., Weiss, M. and Hellman, S. (1992). Effects of noise and noise suppression on speech perception by cochlear implant users. *Ear Hear*., 13: 263-271.

Hornbostel, E. V. and Wertheimer, M. (1920). *Über die Wahrnehmung der Schallrichtung*. Sitzungsberichte der preussischen Akademie der Wissenschaften, 388, 396.

Huang, A. Y. and May, B. J. (1996). Sound orientation behavior in cats. II. Mid-frequency spectral cues for sound localization. *J. Acoust. Soc. Am*., 100(2): 1070-1080.

Huopaniemi, J., Zacharov, N. and Karjalainen, M. (1999). Objective and subjective evaluation of head related transfer function filter design, *J. Audio Eng. Soc*., 47: 218-239.

Iwaki, T., Matsushiro, N., Mah, S., Sato, T., Yasuoka, E., Yamamoto, K. and Kubo, T. (2004). Comparison of speech perception between monaural and binaural hearing in cochlear implant patients. *Acta Otolaryngol*., 124: 358-362.

Jackson, L. B. (1989). Digital Filters and Signal Processing, 2nd ed., Kluwer Academic Publishers, Boston.

Jenison, RL. (1995). A spherical basis function neural network for pole-zero modeling of head-related transfer functions. In: *IEEE Workshop on Applications of Signal Processing to Audio and Acoustics*, 92-95.

Jin, C., Leong, P., Leung, J., Corderoy, A. and Carlile, S. (2000). Enabling individualized virtual auditory space using morphological measurements, In: *Proceedings of the IEEE 2000 International Symposium on Multimedia Information Processing*, 235-238.

Jot, J., Larcher, V. and Warusfel, O. (1995). Digital signal processing issues in the context of binaural and transaural stereophony. In*: Proc. 98th Audio Engr. Soc. Conv.*, Paris, France, preprint 3980.

Kaalund, C. J. and Peng, G. D. (2004). Pole-zero diagram approach to the design of ring resonator-based filters for photonic applications. *J. Lightwave Technology,* 22(6): 1548-1559.

Kistler, D. J. and Wightman, F. L. (1992). A model of head-related transfer functions based on principal components analysis and minimum-phase reconstruction. *J. Acoust. Soc. Am.*, 91(3): 1637-1647.

Koka, K., Read, H. L. and Tollin, D. J. (2008). The acoustical cues to sound location in the rat: Measurements of directional transfer functions. *J. Acoust. Soc. Am.,* 123(6): 4297-4309.

Kreuzer, W., Majdak, P. and Chen, Z. (2009). Fast multipole boundary element method to calculate head-related transfer functions for a wide frequency range. *J. Acoust. Soc. Am.*, 126(3):1280-1290.

Kuhn, G. F. (1987). Acoustics and measurements pertaining to directional hearing. In: *Directional Hearing*, W. A. Yost and G. Gourevitch, Eds., Springer Verlag, New York, 1987, 3-25.

Kulkarni, A. and Colburn, H. S. (1998). Role of spectral detail in sound source localization. *Nature*, London, 396: 747–749.

Kulkarni, A. and Colburn, H. S. (2004). Infinite-impulse-response models of the head-related transfer function. *J. Acoust. Soc. Am.,* 115(4): 1714-1728.

Kulkarni, A., Isabelle, S. K. and Colburn, H. S. (1999). Sensitivity of human subjects to head-related transfer-function phase spectra. *J. Acoust. Soc. Am*., 105(5): 2821-2840.

Laback, B, Pok, S. M., Baumgartner, W. D., Deutsch, W. A. and Schmid, K. (2004). Sensitivity to interaural level and envelope time differences of two bilateral cochlear implant listeners using clinical sound processors. *Ear Hear.*, Oct; 25(5): 488-500.

Langendijk, E. H. and Bronkhorst, A. W. (1997). Collecting localization response with a virtual acoustic pointer. *J. Acoust. Soc. Am*., 101(5): 3106.

Langendijk, E. H. and Bronkhorst, A. W. (2002). Contribution of spectral cues to human sound localization. *J. Acoust. Soc. Am*., 112(4): 1583-1596.

Laske, R., Veraguth, D., Dillier, N., Binkert, A., Holzmann, D., Huber, A. M. (2009). Subjective and objective results after cochlear implantation in adults. *Otol. Neurotol.,* 30: 313-318.

Laszig, R., Aschendorff, A., Stecker, M., Muller-Deile, J., Maune, S., Dillier, N., Weber, B., Hey, M., Begall, K., Lenarz, T., Battmer, R. D., Bohm, M., Steffens, T., Strutz, J., Linder, T., Probst, R., Allum, J., Westhofen, M. and Doering, W. (2004). Benefits of bilateral electrical stimulation with the Nucleus cochlear implant in adults: 6-month postoperative results. *Otol. Neurotol.*, 25: 958-968.

Litovsky, R. Y., Parkinson, A., Arcaroli, J., Peters, R., Lake, J., Johnstone, P. and Yu, G. (2004). Bilateral cochlear implants in adults and children. *Arch. Otolaryngol. Head Neck Surg.*, 130: 648-655.

Litovsky, R. Y., Parkinson, A., Arcaroli, J. and Sammeth, C. (2006). Simultaneous bilateral cochlear implantation in adults: A multicenter study. *Ear Hear.,* 27(6): 714-731.

Litovsky, R. Y., Johnstone, P. M., Godar, S., Agrawal, S., Parkinson, A., Peters, R. and Lake, J. (2006). Bilateral cochlear implants in children: localization acuity measured with minimum audible angle. *Ear Hear.*, 27(1):43-59.

Litovsky, R. Y., Parkinson, A. and Arcaroli, J. (2009). Spatial hearing and speech intelligibility in bilateral cochlear implant users. *Ear Hear.,* 30(4): 419-431.

Liu, C. J. and Hsieh, S. F. (2001). Common-acoustic-poles/zeros approximation of head-related transfer functions. *Acoustics, Speech, and Signal Processing, IEEE International Conference*, 5: 3341-3344.

Lopez-Poveda, E. A. and Meddis, R. (1996). A physical model of sound diffraction and reflections in the human concha. *J. Acoust. Soc. Am.*, 100(5): 3248-3259.

Lorho, G., Huopaniemi, J., Zacharov, N. and Isherwood, D. (2000). Efficient HRTF synthesis using an interaural transfer function model. In: *Proc. EUSIPCO 2000*, 2213-2216.

Lovett, R. E., Kitterick, P. T., Hewitt, C. E. and Summerfield, A. Q. (2010). Bilateral or unilateral cochlear implantation for deaf children: an observational study. *Arch. Dis. Child*, 95: 107-112.

Luntz, M., Shpak, T. and Weiss, H. (2005). Binaural-bimodal hearing: Concomittant use of a unilateral cochlear implant and a contralateral hearing aid. *Acta Oto-Laryngolica*, 125: 863-869.

MacDonald, J. A. (2008). A localization algorithm based on head-related transfer functions. *J. Acoust. Soc. Am*., 123(6): 4290-4296.

Mackenzie, J., Huopaniemi, J., Valimaki, V. and Kale, I. (1997). Low-order modeling of head-related transfer functions using balanced model truncation. *Signal Processing Letters, IEEE*, 4(2): 39-41.

Maki, K. and Furukawa, S. (2005). Acoustical cues for sound localization by the Mongolian gerbil, Merionesunguiculatus. *J. Acoust. Soc. Am*., 118(2): 872-886.

Mallat, S. (1998). A Wavelet Tour of Signal Processing (Academic Press, London).

Martens, W. L. (1987). Principal components analysis and resynthesis of spectral cues to perceived direction. In: *Proc. 1987 Int. Comput. Music Conf*., 274-281.

May, B. J. and Huang, A. Y. (1996). Sound orientation behavior in cats. I. Localization of broadband noise. *J. Acoust. Soc. Am*., 100(2): 1059-1069.

Mehrgardt, S. and Mellert, V. (1977). Transformation characteristics of the external human ear. *J. Acoust. Soc. Am*., 61(6): 1567-1576.

Middlebrooks, J. C. (1992). Narrow-band sound localization related to external ear acoustics. *J. Acoust. Soc. Am*., 92(5): 2607-2624.

Middlebrooks, J. C. (1999a). Virtual localization improved by scaling non-individualized external-ear transfer functions in frequency. *J. Acoust. Soc. Am.*, 106(3): 1493-1510.

Middlebrooks, J. C. (1999b). Individual differences in external-ear transfer functions reduced by scaling in frequency. *J. Acoust. Soc. Am*., 106(3): 1480-1492.

Middlebrooks, J. C., Makous, J. C. and Green, D. M. (1989). Directional sensitivity of sound-pressure levels in the human ear canal. *J. Acoust. Soc. Am.,* 86(1): 89-108.

Miller D. A. and Matin M. A. (2009). A model for simulation of electrically evoked auditory brainstem responses. *Proceedings of Optics and Photonics for Information Processing III*, Vol. 7442:52.

Miller D. A., Matin M. A. (2011). Modeling the head related transfer function for sound localization in normal hearing persons and bilateral cochlear implant recipients. *Proceedings of the 14th ICCIT*, 344-349.

Mok, M., Grayden, D., Dowell, R. and Lawrence, D. (2006). Speech perception for adults who use hearing aids in conjunction with cochlear implants in opposite ears. *J. Speech Lang. Hear. Res*., 49: 338-351.

Morera, C., Manrique, M., Ramos, L., Garcia-Ibanex, L., Cavalle, L., Huarte, A., Castillo, C. and Estrada, E. (2005). Advantages of binaural hearing provided through bimodal stimulation via a cochlear implant and a conventional hearing aid: A 6-month comparative study. *Acta Oto-Laryngologica*, 125: 596-606.

Mosnier, I., Sterkers, O., Bebear, J. P., Godey B., Robier A., Deguine O., Fraysse B., Bordure P., Mondain M., Bouccara D., Bozorg-Grayeli A., Borel S., Ambert-Dahan E., Ferrary E. (2009). Speech performance and sound localization in a complex noisy environment in bilaterally implanted adult patients. *Audiol. Neurotol.*, 14: 106-114.

Muller, J., Schon, F. and Helms, J. (2002). Speech understanding in quiet and noise in bilateral users of the Med-El COMBI 40/40+ cochlear implant system. *Ear Hear.*, 23: 198-206.

Musicant, A. D., and Butler, R. A. (1985). Influence of monaural spectral cues on binaural localization. *J. Acoust. Soc. Am.*, 77(1): 202-208.

Musicant, A. D., Chan, J. C. K. and Hind, J. E. (1990). Direction-dependent spectral properties of cat external ear: New data and cross-species comparisons. *J. Acoust. Soc. Am.,* 87(2): 757-781.

Neuman, A., Haravon, A., Sislian, N., and Waltzman, S. (2007). Sound-direction identification with bilateral cochlear implants. *Ear Hear.*, 28(1), 73-82.

Nishino, T, Kajita, S, Takeda, K, and Itakura, F. (1999). Interpolating head related transfer functions in the median plane. In: *IEEE Workshop on Applications of Signal Process to Audio and Acoustics*, 167-170.

Oppenheim, A. V. and Schafer, R. W. (1975). Digital Signal Processing. Englewood Cliffs, NJ: Prentice-Hall.

Oppenheim, A. V. and Schafer, R. W. (1989). Discrete-time Signal Processing, Prentice-Hall, NJ.

Otani, M. and Ise, S. (2006). Fast calculation system specialized for head-related transfer function based on boundary element method. *J. Acoust. Soc. Am.*, 119(5): 2589-2598.

Otani, M., Iwaya, Y., Suzuki, Y. and Itoh, K. (2010). Numerical analysis of HRTF spectral characteristics based on sound pressures on a pinna surface. *Proceedings of 20th International Congress on Acoustics, ICA 2010,* :1-8.

Papsin, B. C. and Gordon, K. A. (2008). Bilateral cochlear implants should be the standard for children with bilateral sensorineural deafness. *Curr. Opin. Otolaryngol. Head Neck Surg.*, 16(1): 69-74.

Parkinson, A. J., Arcaroli, J., Staller, S. J., Arndt, P. L., Cosgriff, A. and Ebinger, K. (2002). The Nucleus® 24 Contour™ cochlear implant system: Adult clinical trial results. *Ear Hear.*, 23 (Suppl.), 41-48.

Perrott, D. R. and Saberi, K. (1990). Minimum audible angle thresholds for sources varying in both elevation and azimuth. *J. Acoust. Soc.Am.*, 87:1728-1731.

Qi, N. and Li, L. (2011). Acoustic measurement and analysis of different pinna models installed on standard dummy head of chinese adult. In: *IEEE International Conference on Multimedia and Signal Processing (CMSP)*, 2011 Vol. 2: 8-11.

Qu, T., Xiao, Z., Gong, M., Huang, Y., Li, X. and Wu, X. (2008). Distance dependent head-related transfer function database of KEMAR. In: *IEEE International Conference on Audio, Language and Image Processing,* ICALIP 2008: 466-470.

Rao K. R. and Ben-Arie, J. (1996). Optimal head related transfer functions for hearing and monaural localization in elevation: A signal processing design perspective. *IEEE Transactions On Biomedical Engineering*, 43(11):1093-1105.

Raykar, V. C., Duraiswami, R. and Yegnanarayana, B. (2005). Extracting the frequencies of the pinna spectral notches in measured head related impulse responses. *J. Acoust. Soc. Am*., 118(1): 364-374.

Rayleigh, L. (1907). On our perception of sound direction. *Phil. Mag.*, 13: 214-32.

Rice, J. J., Bradford J. M., Spirou, G. A. and Young, E. D. (1992). Pinna-based spectral cues for sound localization in cat. *Hearing Research*, 58(2): 132-152.

Runkle, P. R., Blommer, M. A. and Wakefield, G. H. (1995). A comparison of head related transfer function interpolation methods. In: *IEEE Workshop on Applications of Signal Process to Audio and Acoustics*, 88-91.

Sammeth, C. A., Bundy, S., Miller D. A. (2011). Bimodal hearing devices and bilateral cochlear implants: A review of the research literature. *Seminars in Hearing*, Vol. 32(1): 3-31.

Sandvad, J. and Hammershøi, D. (1994). Binaural auralization: comparison of FIR and IIR filter representation of HIRs. *96th Audio EngrSocConv*, Amsterdam, The Netherlands, preprint 3862. Abstr in: *J. Audio Engr. Soc*., 42: 395.

Scarpaci J. W. and Colburn H. S. (2005). Principal components analysis interpolation of hrtf's using locally chosen basis functions. In: *149th Meeting: Acoustical Society of America*, May 2005. Vancouver, Canada.

Schnupp, J. W. H., Booth, J. and King, A. J. (2003). Modeling individual differences in ferret external ear transfer functions. *J. Acoust. Soc. Am*., 113 (4): 2021-2030.

Searle, C. L., Braida, L. D., Davis, M. F. and Colburn, H. S. (1976). Model for auditory localization. *J. Acoust. Soc. Am*., 60(5): 1164-1175.

Sen, S. and Nehorai, A. (2009). Performance analysis of 3-D direction estimation based on head-related transfer function. *Audio, Speech, and Language Processing, IEEE Transactions on*, 17(4): 607-613.

Senn, P., Kompis, M., Vischer, M. and Haeusler, R. (2005). Minimum audible angle, just noticeable interaural differences and speech intelligibility with bilateral cochlear implants using clinical speech processors. *Audiol. Neurotol*., 10: 342-352.

Shaw, E. A. (1974). Transformation of sound pressure level from the free field to the eardrum in the horizontal plane. *J. Acoust. Soc. Am*., 56(6): 1848-1861.

Shaw, E. A. (1982). External ear response and sound localization. In: *Localization of Sound: Theory and applications*, edited by R. Gatehouse (Amphora, Groton, CT), 30-41.

Shaw, E. A. and Teranishi, R. (1968). Sound pressure in an external ear replica and real human ears by a nearby point source. *J. Acoust. Soc. Am*., 44: 240-249.

Soli, S. D., Jayaraman, S., Gao, S. and Jean, S. (1994). Method of signal processing for maintaining directional hearing with hearing aids, US Patent 5,325,436 (Jun 28, 2004).

Spezio, M. L., Keller, C. H., Marrocco, R. T. and Takahashi, T. T. (2000). Head-related transfer functions of the Rhesus monkey. *Hearing Research* 144(1-2): 73-88.

Steffens, T., Lesinski-Schiedat, A., Strutz, J., Aschendorff A., Klenzner T., Rühl S., Voss B., Wesarg T., Laszig R. and Lenarz T. (2008). The benefits of sequential bilateral cochlear implantation for hearing-impaired children. *Acta Otolaryngol*, 22: 1-13.

Susnik, R., Sodnik, J., Umek, A. and Tomazic, S. (2003). Spatial sound generation using HRTF created by the use of recursive filters. In: *EUROCON 2003. Computer as a Tool. The IEEE Region 8*, vol. 1:449-453.

Tetsufumi, I., Shiro, I. and Hidemi, I. (2000). Pinnae's contribution in head related transfer function (HRTF). *IEIC Technical Report (Institute of Electronics, Information and Communication Engineers)*, Vol. 100; no.725, 153-159.

Tollin, D. J. (2003). The lateral superior olive: A functional role in sound source localization. *Neuroscientist*, 9(2): 127-143.

Tollin, D. J. and Koka, K. (2009). Postnatal development of sound pressure transformations by the head and pinnae of the cat: monaural characteristics. *J. Acoust. Soc. Am.*, 125(2): 980-994.

Tollin, D. J., Populin, L. C., Moore, J. M., Ruhland, J. L. and Yin, T. C. T. (2005). Sound-localization performance in the cat: The effect of restraining the head. *J. Neurophysiol*., 93(3): 1223-1234.

Tollin, D. J. and Yin, T. C. T. (2002). The coding of spatial location by single units in the lateral superior olive of the cat. I. Spatial receptive fields in azimuth. *J. Neurosci.*, 22(4): 1454-1467.

Tyler, R. S., Gantz, B. J., Rubinstein, J. T., Wilson, B. S., Parkinson, A. J., Wolaver, A., Preece, J. P., Witt, S. and Lowder, M. W. (2002). Three-month results with bilateral cochlear implants. *Ear Hear*., 23(Suppl. 1): 80S-89S.

Tyler R. S., Parkinson A. J., Wilson B. S., Witt S., Preece J. P. and Noble W. (2002). Patients utilizing a hearing aid and a cochlear implant: speech perception and localization. *Ear Hear*., 23:98-105.

Tyler, R. S., Dunn, C. C., Witt, S. A. and Preece, J. P. (2003). Update on bilateral cochlear implantation. *Curr. Opin. in Otolaryngol. Head and Neck Surgery*, 11(5): 388-393.

Tyler, R. S., Dunn, C. C., Witt, S. A. and Noble, W. G. (2007). Speech perception and localization with adults with bilateral sequential cochlear implants. *Ear and Hearing*, 28(2), 86S-90S.

Van Deun, L., van Wieringen, A., Scherf, F., Deggouj N., Desloovere C., Offeciers F. E., Van de Heyning P. H., Dhooge I. J. and Wouters J. (2010). Earlier intervention leads to better sound localization in children with bilateral cochlear implants. *Audiol. Neurotol.*, 15: 7-17.

van Hoesel, R. J. M., Tong, Y. C., Hollow, R. D. and Clark, G. M. (1993). Psychophysical and speech perception studies: A case report on a binaural cochlear implant subject. *J. Acoust. Soc. Amer*., 94: 3178-3189.

van Hoesel, R. J. M. and Clark, G. M. (1995). Fusion and lateralization study with two binaural cochlear implant patients. *Ann. Otol. Rhinol. Laryngol*., 104 (Suppl. 166): 233-235.

van Hoesel, R. J. M. and Clark, G. M. (1997). Psychophysical studies with two binaural cochlear implant subjects. *J. Acoust. Soc. Amer*., 102: 495-507.

van Hoesel, R. J. M., Ramsden, R. and O'Driscoll, M. (2002). Sound direction identification, interaural time delay discrimination, and speech intelligibility advantages in noise for a bilateral cochlear implant user. *Ear Hear*, 23:137-149.

van Hoesel, R. J. M. and Tyler, R. (2003). Speech perception, localization, and lateralization with bilateral cochlear implants. *J. Acoust. Soc. Amer*., 113(3):1617–1630.

van Hoesel, R. J. M. (2004). Exploring the benefits of bilateral cochlear implants. *Audiol. Neurootol*., 9(4): 234-246.

Verschuur, C. A., Lutman, M. E., Ramsden, R., Greehan, P. and O'Driscoll, M. (2005). Auditory localization abilities in bilateral cochlear implant recipients. *Otol. Neurol.*, 26: 965-971.

Vondrasek, M., Sovka, P. and Tichy, T. (2008). ACE Strategy with virtual channels. *Radioengineering*, 17(4):55-61.

Wenzel, E. M. and Foster, S. H. (1993). Perceptual consequences of interpolating head-related transfer functions during spatial synthesis. In: *IEEE Workshop on Applications of Signal Process to Audio and Acoustics, Final Program and Paper Summaries*, 102-105.

Wenzel, E. M., Arruda, M., Kistler, D. J. and Wightman, F. L. (1993). Localization using nonindividualized head-related transfer functions. *J. Acoust. Soc. Amer*., 94(1): 111-123.

Wesley, G. D., Willhite, J. A., Frampton, K. D. and Ashmead, D. H. (2005). Reduced order modeling of head related impulse responses for virtual acoustic displays. *J. Acoust. Soc. Amer*., 117(5): 3116-3125.

Wightman, F. L. and Kistler, D. J. (1989a). Headphone simulation of free-field listening. I: Stimulus synthesis. *J. Acoust. Soc. Amer*., 85(2): 858-867.

Wightman, F. L., and Kistler, D. J. (1989b). Headphone simulation of free-field listening. II: Psychophysical validation. *J. Acoust. Soc. Amer.,* 85(2): 868-878.

Wightman, F. L. and Kistler, D. J. (1999). Explaining individual differences in head-related transfer functions. *J. Acoust. Soc. Am*., 105(2): 1036.

Wilson B. S., Lawson D. T., Muller J. M., Tyler R. S. and Kiefer J. (2003). Cochlear implants: Some likely next steps. *Annu Rev Biomed Eng,* 5:207-249.

Wilson, B. S. and Dorman, M. F. (2008). Cochlear implants: current designs and future possibilities. *J. Rehabil. Res. Dev.*, 45(5), 695-730.

Yost, W. and Dye, R. (1997). Fundamentals of directional hearing. *Sem. Hear*., 18: 321-344.

Young, E. D., Spirou, G. A., Rice, J. J. and Voigt, H. F. (1992). Neural organization and responses to complex stimuli in the dorsal cochlear nucleus. *Philos. Trans. R. Soc. Lond. B. Biol. Sci*., B 336(1278): 407–413.

Zurek, P (1993). Binaural advantages and direction effects in speech intelligibility. In: Studebaker, GA, Hochberg, I (Eds.). *Acoustical Factors Affecting Hearing Aid Performance,* 2nd Ed. Boston: Allyn & Bacon, 255-276.

Appendices

1. MATLAB Code: Main Module

```
%                  Spatial Localization Algorithm
%
% Determines the direction a signal is emanating from using binaural
% hearing.  The signal is picked up at two locations spaced at the
% width of the head centered at the origin.  Signal source data was
% obtained from a KEMAR manikin.  A basic and common cochlear implant
% algorithm is used when hearing is set to ci.

clc                                     % clear command window
clear                                   % clear variables
hearing = 'normal';                     % select 'normal' or 'ci'

azimuth = 030;                          % select signal source azimuth
phi     = 000;                          % select signal source
elevation
at      = 6.6;                          % anterior threshold constant

if azimuth > 95  i = 9;                 % set source data index value
elseif azimuth > 5  i = 10;
else  i = 11;
end

filename = 'Data\L0e000a.wav';          % create source data file name
filename(i:11) = num2str(azimuth);

% read signal data
[x1,fs] = wavread(filename);            % extract signal 1
if azimuth > 0 azimuth2 = 360 - azimuth; % select signal 2
else azimuth2 = 0;
end
filename(9:11) = num2str(azimuth2);
[x2,fs] = wavread(filename);            % extract signal 2
[samples,row] = size(x1);               % number of samples read

% normal hearing pinna effects
if strcmp(hearing, 'nornal')            % normal hearing selected
    x1 = pinna(x1, azimuth, phi);
    x2 = pinna(x2, azimuth, phi);
end
```

```
% ci signal processing
if strcmp(hearing, 'ci')                % cochlear implant selected
    x1 = cidsp(x1,13,17);
    x2 = cidsp(x2,13,17);
    at = at * hearing(2)/100;
end

% plot signals
figure;
subplot(2,1,1), plot(x1,'b');           % plot signal 1
axis([0 samples -1 1])
title('Signal [Left Ear]');
subplot(2,1,2), plot(x2,'r');           % plot signal 2
axis([0 samples -1 1])
title('Signal [Right Ear]');

% perform Fourier transform
n = 2048;                               % set FFT size
y1 = fft(x1,n);                         % compute the FFT of signal 1
y1 = y1(1:n/2);                         % take the first
half
m1 = abs(y1);                           % magnitude of signal 1
p1 = unwrap(angle(y1));                 % phase of signal 1

y2 = fft(x2,n);                         % compute the FFT of signal 2
y2 = y2(1:n/2);                         % take the first
half
m2 = abs(y2);                           % magnitude of signal 2
p2 = unwrap(angle(y2));                 % phase of signal 2

if max(m1) > max(m2)                    % get index of maximum
magnitude
    [C,i] = max(m1);
else
    [C,i] = max(m2);
end

Magnitude1 = m1(i);
Phase1 = 360*p1(i)/6.2832;              % convert phase to degrees
Magnitude2 = m2(i);
Phase2 = 360*p2(i)/6.2832;              % convert phase to degrees
dPhase = Phase2 - Phase1;               % compute phase delay

% plot spectrum
f = (0:0.5*n-1)*fs/n;                   % calculate values in Hertz

figure;
subplot(2,1,1);
plot(f,m1,'b',f,m2,'r');                % plot magnitudes
v = axis;                               % get axis limits
axis([0 10000 -5 1.5*v(4)])
title('Spectrum Magnitude');
ylabel('Abs. Magnitude'), grid on;
```

```
xlabel('Frequency [Hz]');

subplot(2,1,2);
plot(f,p1*180/pi,'b',f,p2*180/pi,'r');    % plot phase in degrees
v = axis;                                 % get axis limits
axis([0 10000 v(3) v(4)])
title('Spectrum Phase');
ylabel('Phase [Degrees]'), grid on;
xlabel('Frequency [Hz]');

% determine direction to target
c = 343; %meters/second                     speed of sound
d = 0.2; %meters                            distance between ears
itd = abs(dPhase/(360*f(i))); %seconds      interaural time delay
Cf = -1205475*itd^2 + 590*itd + 1;        % head shadow coefficient
temp = Cf*c*itd/d;
theta_d = 180*asin(Cf*c*itd/d)/pi; %deg     calculate angle to target
[deg]
theta_r = asin(Cf*c*itd/d); %rad            calculate angle to target
[rad]

if (Magnitude1 + Magnitude2 < at)         % check for signal from behind
    AP = 180; %°/rad                        anterior position in degrees
    APr = AP/360 * 2 * pi;                % anterior position in radians
    theta_d = AP-180*asin(Cf*c*itd/d)/pi;% angle to target if anterior
    theta_r = APr-asin(Cf*c*itd/d);
end

% plot direction to target
figure;
polar([0 theta_r],[0 1],'-r');
title('Angle to Target');
% display detected azimuth angle
theta_d

% push data into arrays for analysis
FFT_array( 1+azimuth/5 , 1 ) = y1(i);
FFT_array( 1+azimuth/5 , 2 ) = y2(i);

azimuth_data(1+azimuth/5, 1) = azimuth;
azimuth_data(1+azimuth/5, 2) = theta_d;
azimuth_data(1+azimuth/5, 3) = itd;
azimuth_data(1+azimuth/5, 4) = dPhase;
```

2. MATLAB Code: Iteration Module

```
%        Spatial Localization Algorithm - Rotating Azimuth
%
% Determines the direction a signal is emanating from using binaural
% hearing.  Iterative algorithm that computes the localization values
% as the signal is rotated about the head.  The RMS Error is also
% calculated for the detected location.  A basic and common cochlear
% implant algorithm is used when hearing is set to ci.

clc                                     % clear command window
clear                                   % clear variables
hearing = 'ci';                         % select 'normal' or 'ci'

for a = 0:36;

azimuth = a*5;                          % select source data set
phi     = 000;                          % select signal source
elevation
at      = 6.6;                          % anterior threshold constant

if azimuth > 95  i = 9;                 % set source data index value
elseif azimuth > 5  i = 10;
else  i = 11;
end

filename = 'Data\L0e000a.wav';          % create source data file name
filename(i:11) = num2str(azimuth);

% read signal data
[x1,fs] = wavread(filename);            % extract signal 1
if azimuth > 0 azimuth2 = 360 - azimuth; % select signal 2
else azimuth2 = 0;
end
filename(9:11) = num2str(azimuth2);
[x2,fs] = wavread(filename);            % extract signal 2
[samples,row] = size(x1);               % number of samples read

% normal hearing pinna effects
if strcmp(hearing, 'nornal')            % normal hearing selected
    x1 = pinna(x1, azimuth, phi);
    x2 = pinna(x2, azimuth, phi);
end

% ci signal processing
if strcmp(hearing, 'ci')                % cochlear implant selected
    x1 = cidsp(x1,13,17);
    x2 = cidsp(x2,13,17);
    at = at * hearing(2)/100;
end

% perform Fourier transform
n = 2048;                               % set FFT size
```

```
y1 = fft(x1,n);                         % compute the FFT of signal 1
y1 = y1(1:n/2);                         % take the first
half
m1 = abs(y1);                           % magnitude of signal 1

y2 = fft(x2,n);                         % compute the FFT of signal 2
y2 = y2(1:n/2);                         % take the first
half
m2 = abs(y2);                           % magnitude of signal 2

if max(m1) > max(m2)                    % get index of maximum
magnitude
    [C,i] = max(m1);
else
    [C,i] = max(m2);
end

p1 = unwrap(angle(y1));                 % phase of signal 1
Magnitude1 = m1(i);
Phase1 = 360*p1(i)/6.2832;              % convert phase to degrees
p2 = unwrap(angle(y2));                 % phase of signal 2
Magnitude2 = m2(i);
Phase2 = 360*p2(i)/6.2832;              % convert phase to degrees
dPhase = Phase2 - Phase1;               % compute phase delay

% plot spectrum
f = (0:0.5*n-1)*fs/n;                   % calculate values in Hertz

% determine direction to target
c = 343; %meters/second                 % speed of sound
d = 0.2; %meters                        % distance between ears
itd = abs(dPhase/(360*f(i))); %seconds  % interaural time delay
if itd>0.001 itd = itd/2; end
Cf = -1205475*itd^2 + 590*itd + 1;      % head shadow coefficient
temp = Cf*c*itd/d;
theta_d = 180*asin(Cf*c*itd/d)/pi; %deg   calculate angle to target
[deg]
theta_r = asin(Cf*c*itd/d); %rad        % calculate angle to target
[rad]

if (Magnitude1 + Magnitude2 < at)       % check for signal from behind
    AP = 180; %°/rad                      anterior position in degrees
    APr = AP/360 * 2 * pi;              % anterior position in radians
    theta_d = AP-180*asin(Cf*c*itd/d)/pi;% angle to target if anterior
    theta_r = APr-asin(Cf*c*itd/d);
    flag = 1;
end

progressbar(a/36);

% push data into arrays for analysis
azimuth_data(1+azimuth/5, 1) = azimuth;
azimuth_data(1+azimuth/5, 2) = theta_d;
azimuth_data(1+azimuth/5, 3) = itd;
```

```
azimuth_data(1+azimuth/5, 4) = dPhase;

FFT_data(1+azimuth/5, 1) = Magnitude1;
FFT_data(1+azimuth/5, 2) = Phase1;
FFT_data(1+azimuth/5, 3) = Magnitude2;
FFT_data(1+azimuth/5, 4) = Phase2;

FFT_Phase(:, 1+azimuth/5) = p2;
FFT_Mag(1+azimuth/5, :) = m1;
end

% plot error and calculate the RMS Error value for all azimuths
figure;
rmsE = sqrt(mse(azimuth_data(:,1)-azimuth_data(:,2)));
plot(azimuth_data(:,1),azimuth_data(:,1),'k',...
     azimuth_data(:,1),azimuth_data(:,2),'r');
text(40,160,['RMS Error:
',num2str(rmsE)],'HorizontalAlignment','center');
```

3. MATLAB Code: Cochlear Implant Processing Module

```
%              Cochlear Implant Processing Algorithm
%
% This function is used to apply a basic,but typical cochlear implant
% signal processing algorithm to the incoming signal.  This function
% replaces the pinna effect function, as the signal is received by the
% cochlear implant microphone rather than the ear.

function [x_out] = cidsp(x_in,lb,ub)

% filter boundaries used in a commonly used cochlear implant
filterbank = [188 313 438 563 688 813 938 1063 1188 1313 1563 1813 ...
              2063 2313 2688 3063 3563 4063 4688 5313 6063 6938 7938];

% set filter parameters
m = 22000; %Hz                              signal bandwidth
sk = 990; %Hz                               filter skirt width
pl = filterbank(lb); %Hz                    passband lower limit
pu = filterbank(ub); %Hz                    passband upper limit
lb = pl - sk;
ub = pu + sk;

% generate the filter
ftype = 'Fst1,Fp1,Fp2,Fst2,Ast1,Ap,Ast2';
d = fdesign.bandpass(ftype,lb/m,pl/m,pu/m,ub/m,60,1,60);
Hd = design(d,'equiripple');

% apply ci processing to the signal
x_out = filter(Hd,x_in);
```

4. MATLAB Code: Pinna Module

```
%                       Pinna Effects
%
% This function is used to process pinna effects
% on the incoming signal and thus account for the
% filtering component introduced by the idealized
% human pinna.

function [x_out] = pinna(x_in, azimuth, elevation)

% convert azimuth and elevation to radians
theta = (azimuth/360) * 2 * pi;
phi = (elevation/360) * 2 * pi;

% set delay constant values
A = [0 1 5 5 5 5];
B = [0 2 4 7 11 13];
C = 0.5;
D = [0 1 0.5 0.5 0.5 0.5];

tau = zeros(6,1);
theta = asin(abs(sin(theta)));

% calculate the delay for each pinna echo
for n = 2:6
    tau(n) = A(n) * cos(C*theta)*sin(D(n)*(pi/2 - phi)) + B(n);
end

% magnitude of each pinna echo
rho = [1 0.5 -1 0.5 -0.25 0.25];
h = zeros(32,1)';
h(1) = 1;

% generate a 32-tap impulse response filter to represent the pinna
echos
for n = 2:6
    t2 = ceil(tau(n));
    t1 = t2-1;

    if(t2 < 32)
        h(t2) = h(t2) + rho(n) * (tau(n) - t1);
        h(t1) = h(t1) + rho(n) * (tau(n) - t2);
    end
end

% apply the pinna echo effects
echos = conv(x_in, h);

% apply a smoothing filter
[b,a] = butter(1, 3000/22050);
```

```
% return the filtered signal back to the main routine
x_out = filter(b,a,echos);
```

5. List of Publications and Presentations

Miller D. A. and Matin M. A. (2013). A model for predicting localization performance in cochlear implant users. *W J Neuroscience*, Accepted June 2013.

Miller D. A. and Matin M. A. (2011). Modeling the head related transfer function for sound localization in normal hearing persons and bilateral cochlear implant recipients. *Proceedings of the 14th ICCIT*, 344-349.

Miller D. A. and Matin M. A. (2011). Modeling the head related transfer function for sound localization in normal hearing persons and bilateral cochlear implant recipients. *Presented at the 14th International Conference on Computer and Information Technology*, 22-24 December, 2011.

Miller D. A. and Matin M. A. (2011). Localization model for cochlear implants. *Proceedings of SPIE OP 2011*, Vol. 8134:07.

Sammeth, C. A., Bundy, S., and **Miller D. A.** (2011). Bimodal hearing devices and bilateral cochlear implants: A review of the research literature. *Seminars in Hearing*, Vol. 32(1): 3-31.

Miller D. A. and Matin M. A. (2011). Localization model for cochlear implants. *Presented at 2011 Optics + Photonics: Nanoscience + Engineering*. San Diego, 21-25 August 2011.

Miller D. A. and Matin M. A. (2009). A model for simulation of electrically evoked auditory brainstem responses. *Proceedings of Optics and Photonics for Information Processing III*, Vol. 7442:52.

Miller D. A. and Matin M. A. (2009). A model for simulation of electrically-evoked auditory brainstem responses. *Presented at the Society of Photo-Optical Instrumentation Engineers Conference*, San Diego, 2009.